



**AIAA-93-3359**

**Artificial Diffusion, Upwind Biasing,  
Limiters and their Effect on  
Accuracy and Multigrid Convergence  
in Transonic and Hypersonic Flows**

A. Jameson

Princeton University

Princeton, NJ

**11th AIAA Computational Fluid  
Dynamics Conference**

**July 6–9, 1993 / Orlando, FL**

# Artificial Diffusion, Upwind Biasing, Limiters and their Effect on Accuracy and Multigrid Convergence in Transonic and Hypersonic Flows

*Antony Jameson*

Department of Mechanical and Aerospace Engineering  
Princeton University  
Princeton, New Jersey 08544 USA

## Abstract

The theory of non-oscillatory scalar schemes is developed in this paper in terms of the local extremum diminishing (LED) principle that maxima should not increase and minima should not decrease. This principle can be used for multi-dimensional problems on both structured and unstructured meshes, while it is equivalent to the total variation diminishing (TVD) principle for one-dimensional problems. A new formulation of symmetric limited positive (SLIP) schemes is presented, which can be generalized to produce schemes with arbitrary high order of accuracy in regions where the solution contains no extrema, and which can also be implemented on multi-dimensional unstructured meshes. Systems of equations lead to waves traveling with distinct speeds and possibly in opposite directions. Alternative treatments using characteristic splitting and scalar diffusion fluxes are examined, together with a modification of the scalar diffusion through the addition of pressure differences to the momentum equations to produce full upwinding in supersonic flow. This convective upwind and split pressure (CUSP) scheme exhibits very rapid convergence in multigrid calculations of transonic flow, and provides excellent shock resolution at very high Mach numbers.

## 1 Introduction

Over the past decade the principles underlying the design of non-oscillatory discretization schemes for compressible flows have been quite well established. A very large number of variations of artificial dif-

fusion, upwind biasing and flux splitting have been proposed and tested [12, 20, 14, 17, 16, 5, 22, 9]. In the same period multigrid acceleration schemes have also been the subject of widespread investigation, and have proved effective, particularly for subsonic and transonic flow. This paper presents some new variations of artificial diffusion and flux limiters which achieve high resolution of shock waves without oscillation. At the same time fast convergence is obtained with multigrid in both transonic and hypersonic flow.

Two main issues arise in the design of non-oscillatory discrete schemes. First there is the issue of how to construct an approximation to a scalar convection or convection-diffusion equation which is non-oscillatory, captures discontinuities with high resolution, and is sufficiently accurate. Second there is the issue of how to construct a numerical flux for a system of equations with waves traveling at different speeds, and sometimes in opposite directions.

The next section reviews the conditions for the construction of non-oscillatory schemes for scalar nonlinear conservation laws. It is suggested that the principle of non increasing maxima and non decreasing minima provides a convenient criterion for the design of non-oscillatory schemes. This principle contains the concept of total variation diminishing (TVD) schemes for one-dimensional problems, but can be readily applied to multi-dimensional problems with both structured and unstructured grids. Such local extremum diminishing (LED) schemes can be realized by making sure that the coefficients of the discrete approximation are non-negative. First order schemes satisfying this crite-

tion are easily constructed but are too diffusive. A simple and effective way of introducing limited anti-diffusive terms is presented. This leads to a new class of symmetric limited positive (SLIP) schemes that provide high resolution of shock waves, and can be implemented on both structured and unstructured grids. These schemes can be generalized to attain any desired order of accuracy in regions where the solution has no extrema.

Section 3 discusses the treatment of systems of equations with several dependent variables. In order to apply the local extremum diminishing (LED) principle, the flux may be split in a manner which corresponds to the characteristic fields, so that the scheme is designed to limit extrema of the characteristic variables. The Roe flux [17] provides a way to produce schemes that resolve stationary shock waves with a single interior point. The use of a scalar diffusive flux constructed directly from the solution variables leads to simpler schemes which can resolve shock waves with several interior points, and exhibit no overshoots provided that enough diffusion is introduced locally. These schemes have proved quite effective for steady state calculations. Very rapid convergence to a steady state can be achieved by the introduction of multigrid acceleration techniques. Because of their low computational costs these schemes are suitable for industrial use, and they have been successfully used for aerodynamic analysis in the design of aircraft such as the YF-23 [3].

Scalar diffusion has the drawbacks that it is less effective in resolving moving shockwaves, and that in order to stabilize the calculation it tends to introduce more diffusion than is really needed. This can lead to a degradation of accuracy, for example, in the treatment of viscous flows where the numerical diffusion in the boundary layer should be kept as small as possible. In supersonic flow the region of dependence is purely upstream, while the use of scalar diffusion cannot produce a discrete scheme which is fully upwinded. This can be remedied by the introduction of pressure differences in the momentum equation. It is then possible to construct a first order scheme which reduces to pure upwinding in supersonic flow, and which may be used as the basis for constructing higher order schemes. Upwinding of the pressure requires the introduction of terms

which may be related to the flux splitting recently proposed by Liou and Steffen [15]. This simple convective upwind and split pressure (CUSP) scheme produces discrete normal shock waves which contain two or three interior points in transonic flow, and becomes sharper at very high Mach numbers.

Since the solution variables may develop new extrema, limiters may have an adverse effect if they are applied globally in conjunction with the scalar or CUSP diffusive fluxes. With the CUSP scheme it has been found that excellent oscillation control is achieved by a switch between first and third order diffusion of the type introduced by Jameson *et al.* [12], and generalized by Swanson and Turkel [21].

Section 4 presents results of various test calculations for one-, two- and three-dimensional problems. It is verified that the SLIP scheme with Roe flux provides high resolution of shock waves in shock tube simulations. It also produces shock waves with one interior point in steady transonic flow calculations for airfoils. The rate of convergence to steady state is significantly faster with the CUSP scheme. Transonic solutions using the CUSP scheme on a  $160 \times 32$  grid are presented for three different airfoils. Each was obtained in 12 multigrid W-cycles with a multi-stage explicit time stepping scheme. The reduction of the number of steps needed for global convergence to 12 is the culmination of 12 years of effort.

## 2 Non-oscillatory schemes for scalar equations

### 2.1 Local extremum diminishing (LED) schemes with positive coefficients

Consider the discretization of a time dependent conservation law such as

$$\frac{\partial v}{\partial t} + \frac{\partial}{\partial x} f(v) + \frac{\partial}{\partial y} g(v) = 0, \quad (1)$$

for a scalar dependent variable  $v$  on an arbitrary (possibly unstructured) mesh. Assuming that the mesh points are numbered in some way, let  $v_j$  be the value at mesh point  $j$ . Suppose that the approximation to (1) can be expressed in semi-discrete form in terms of differences between  $v_j$  and other

mesh values  $v_k$  as

$$\frac{dv_j}{dt} = \sum_k c_{kj} (v_k - v_j).$$

If the scheme is supported by a compact stencil of points,  $c_{kj}$  will be zero for most values of  $k$ . Let the coefficients satisfy the positivity condition

$$c_{kj} \geq 0. \quad (2)$$

Then if  $v_j$  is a local maximum (over the stencil of the difference scheme)  $v_k - v_j \leq 0$ , with the consequence that  $\frac{dv_j}{dt} \leq 0$ . Thus a local maximum cannot increase, and similarly a local minimum cannot decrease. Such a scheme will be called local extremum diminishing (LED).

This criterion was proposed by the author [8, 9, 11] as a convenient basis for the construction of non-oscillatory schemes on unstructured meshes. It assures positivity, because if  $v$  is everywhere positive, then its global minimum is positive, and this cannot decrease. When specialized to one dimension it also leads to the class of total variation diminishing (TVD) schemes proposed by Harten [5]. The total variation of  $v$  is

$$TV(v) = \int_{-\infty}^{\infty} \left| \frac{dv}{dx} \right| dx,$$

that is the sum of the absolute values of the variation over each upward and downward segment. It was observed by Laney and Caughey [13] that each extremum appears in the variation of the segment on each side of that extremum, with the consequence that

$$TV(v) = 2 \left( \sum \text{maxima} - \sum \text{minima} \right),$$

if the end values are fixed. Thus, if a one-dimensional scheme is LED, it is also TVD. However, the TVD criterion does not readily generalize to multi-dimensional problems, whereas the LED criterion can be directly applied to multi-dimensional problems on both structured and unstructured meshes.

If the one-dimensional scalar conservation law

$$\frac{\partial v}{\partial t} + \frac{\partial}{\partial x} f(v) = 0 \quad (3)$$

is represented by a three point scheme

$$\frac{dv_j}{dt} = c_{j+\frac{1}{2}}^+ (v_{j+1} - v_j) + c_{j-\frac{1}{2}}^- (v_{j-1} - v_j),$$

the scheme is LED if

$$c_{j+\frac{1}{2}}^+ \geq 0, \quad c_{j-\frac{1}{2}}^- \geq 0. \quad (4)$$

Suppose that (3) is approximated in conservation form by the semi-discrete scheme

$$\Delta x \frac{dv_j}{dt} + (h_{j+\frac{1}{2}} - h_{j-\frac{1}{2}}) = 0, \quad (5)$$

where  $h_{j+\frac{1}{2}}$  is the numerical flux between cells  $j$  and  $j+1$ , and  $\Delta x$  is the mesh interval. In a diffusive scheme  $h_{j+\frac{1}{2}}$  may be calculated as

$$h_{j+\frac{1}{2}} = \frac{1}{2} (f_{j+1} + f_j) - \alpha_{j+\frac{1}{2}} (v_{j+1} - v_j),$$

where the second term is a diffusive flux of first order. If the wave speed  $a(v) = \frac{\partial f}{\partial v}$  is approximated as

$$a_{j+\frac{1}{2}} = \begin{cases} \frac{f_{j+1} - f_j}{v_{j+1} - v_j}, & v_{j+1} \neq v_j \\ \left. \frac{\partial f}{\partial v} \right|_{v_j}, & v_{j+1} = v_j \end{cases},$$

then

$$\begin{aligned} h_{j+\frac{1}{2}} - h_{j-\frac{1}{2}} &= + \left( \frac{1}{2} a_{j+\frac{1}{2}} - \alpha_{j+\frac{1}{2}} \right) \Delta v_{j+\frac{1}{2}} \\ &\quad + \left( \frac{1}{2} a_{j-\frac{1}{2}} + \alpha_{j-\frac{1}{2}} \right) \Delta v_{j-\frac{1}{2}}, \end{aligned}$$

where

$$\Delta v_{j+\frac{1}{2}} = v_{j+1} - v_j.$$

Thus the LED condition (4) is satisfied if

$$\alpha_{j+\frac{1}{2}} \geq \frac{1}{2} |a_{j+\frac{1}{2}}|. \quad (6)$$

If one takes

$$\alpha_{j+\frac{1}{2}} = \frac{1}{2} |a_{j+\frac{1}{2}}|,$$

the diffusive flux becomes

$$d_{j+\frac{1}{2}} = \frac{1}{2} |a_{j+\frac{1}{2}}| \Delta v_{j+\frac{1}{2}}$$

and one obtains the first order upwind scheme

$$h_{j+\frac{1}{2}} = \begin{cases} f_j & \text{if } a_{j+\frac{1}{2}} > 0 \\ f_{j+1} & \text{if } a_{j+\frac{1}{2}} < 0 \end{cases}.$$

This is the least diffusive first order scheme which satisfies the LED condition. In this sense upwinding is a natural approach to the construction of non-oscillatory schemes.

## 2.2 High resolution switched Jameson-Schmidt-Turkel (JST) scheme

Higher order non-oscillatory schemes are generally derived by introducing anti-diffusive terms in a controlled manner. Anti-diffusive terms can be introduced by subtracting neighboring differences to produce a third order diffusive flux

$$d_{j+\frac{1}{2}} = \alpha_{j+\frac{1}{2}} \left\{ \Delta v_{j+\frac{1}{2}} - \frac{1}{2} (\Delta v_{j+\frac{3}{2}} + \Delta v_{j-\frac{1}{2}}) \right\} \quad (7)$$

The positivity condition (2) is violated by this scheme. It generates substantial oscillations in the vicinity of shock waves which can be eliminated by switching locally to the first order scheme. The switch introduced by Jameson, Schmidt and Turkel [12], which has proved effective for this purpose, has recently been improved by Swanson and Turkel [21]. The improved switch is taken as the maximum in some neighborhood of

$$Q_j = \left| \frac{\Delta v_{j+\frac{1}{2}} - \Delta v_{j-\frac{1}{2}}}{P_0 + (1-\epsilon)P_1 + \epsilon P_2} \right|,$$

where

$$\begin{aligned} P_1 &= |\Delta v_{j+\frac{1}{2}}| + |\Delta v_{j-\frac{1}{2}}| \\ P_2 &= |v_{j+1}| + 2|v_j| + |v_{j-1}|. \end{aligned} \quad (8a)$$

The value of  $\epsilon$  is typically  $\frac{1}{2}$ , and  $P_0$  is a threshold to make sure that the denominator cannot be zero. Other quantities such as the entropy may be used to calculate the switch. The diffusive flux is now calculated as

$$\begin{aligned} d_{j+\frac{1}{2}} &= +\epsilon_{j+\frac{1}{2}}^{(2)} \Delta v_{j+\frac{1}{2}} \\ &\quad - \epsilon_{j+\frac{1}{2}}^{(4)} \left( \Delta v_{j+\frac{3}{2}} - 2\Delta v_{j+\frac{1}{2}} + \Delta v_{j-\frac{1}{2}} \right), \end{aligned} \quad (8b)$$

where if  $S$  is the maximum of  $Q$  in a neighborhood, then

$$\begin{aligned} \epsilon_{j+\frac{1}{2}}^{(2)} &= \min(\alpha_1, \alpha_2 S) |a_{j+\frac{1}{2}}| \\ \epsilon_{j+\frac{1}{2}}^{(4)} &= \max\left(0, \beta_1 - \beta_2 \epsilon_{j+\frac{1}{2}}^{(2)}\right) |a_{j+\frac{1}{2}}|. \end{aligned} \quad (8c)$$

Usually  $\alpha_1 = \frac{1}{2}$ ,  $\beta_1 = \frac{1}{4}$  to scale the diffusion to the level corresponding to upwinding, while  $\alpha_2$  and  $\beta_2$  must be chosen to switch from third order to first order diffusion fast enough near a shock wave.

## 2.3 Symmetric limited positive (SLIP) scheme

An alternative route to high resolution without oscillation is to introduce flux limiters to guarantee the satisfaction of the positivity condition (2). The use of limiters dates back to the work of Boris and Book [2]. A particularly simple way to introduce limiters, proposed by the author in 1984 [7], is to use flux limited dissipation. In this scheme the third order diffusion defined by equation (7) is modified by the insertion of limiters which produce an equivalent three point scheme with positive coefficients. The original scheme can be improved in the following manner so that less restrictive flux limiters are required. Let  $L(u, v)$  be a limited average of  $u$  and  $v$  with the following properties:

$$P1. L(u, v) = L(v, u)$$

$$P2. L(\alpha u, \alpha v) = \alpha L(u, v)$$

$$P3. L(u, u) = u$$

$$P4. L(u, v) = 0 \text{ if } u \text{ and } v \text{ have opposite signs}$$

Properties (P1-P3) are natural properties of an average. Property P4 is needed for the construction of an LED or TVD scheme.

It is convenient to introduce the notation

$$\phi(r) = L(1, r) = L(r, 1).$$

Then it follows from (P2) that

$$L(u, v) = \phi\left(\frac{v}{u}\right) u = \phi\left(\frac{u}{v}\right) v.$$

Also it follows on setting  $v = 1$  and  $u = r$  that

$$\phi(r) = r\phi\left(\frac{1}{r}\right).$$

Thus, if there exists  $r < 0$  for which  $\phi(r) > 0$ , then  $\phi\left(\frac{1}{r}\right) < 0$ . The only way to ensure that  $\phi(r) \geq 0$  is to require  $\phi(r) = 0$  for all  $r < 0$ , corresponding to property P4.

Now one defines the diffusive flux for a scalar conservation law as

$$d_{j+\frac{1}{2}} = \alpha_{j+\frac{1}{2}} \left\{ \Delta v_{j+\frac{1}{2}} - L\left(\Delta v_{j+\frac{3}{2}}, \Delta v_{j-\frac{1}{2}}\right) \right\} \quad (9)$$

Also define

$$r^+ = \frac{\Delta v_{j+\frac{3}{2}}}{\Delta v_{j-\frac{1}{2}}}, \quad r^- = \frac{\Delta v_{j-\frac{3}{2}}}{\Delta v_{j+\frac{1}{2}}}.$$

Then, the scalar scheme (5) reduces to

$$\begin{aligned} \Delta x \frac{dv_j}{dt} &= -\frac{1}{2}a_{j+\frac{1}{2}}\Delta v_{j+\frac{1}{2}} - \frac{1}{2}a_{j-\frac{1}{2}}\Delta v_{j-\frac{1}{2}} \\ &\quad + \alpha_{j+\frac{1}{2}} \left( \Delta v_{j+\frac{1}{2}} - \phi(r^+) \Delta v_{j-\frac{1}{2}} \right) \\ &\quad - \alpha_{j-\frac{1}{2}} \left( \Delta v_{j-\frac{1}{2}} - \phi(r^-) \Delta v_{j+\frac{1}{2}} \right) \\ &= + \left\{ \alpha_{j+\frac{1}{2}} - \frac{1}{2}a_{j+\frac{1}{2}} + \alpha_{j-\frac{1}{2}}\phi(r^-) \right\} \Delta v_{j+\frac{1}{2}} \\ &\quad - \left\{ \alpha_{j-\frac{1}{2}} + \frac{1}{2}a_{j-\frac{1}{2}} + \alpha_{j+\frac{1}{2}}\phi(r^+) \right\} \Delta v_{j-\frac{1}{2}} \end{aligned}$$

Thus the scheme satisfies the LED condition if  $\alpha_{j+\frac{1}{2}} \geq \frac{1}{2}|a_{j+\frac{1}{2}}|$  for all  $j$ , and  $\phi(r) \geq 0$ , which is assured by property (P4) on  $L$ . At the same time it follows from property (P3) that the first order diffusive flux is canceled when  $\Delta v$  is smoothly varying and of constant sign. A variation is to include the coefficient  $\alpha_{j+\frac{1}{2}}$  in the limited average by setting

$$d_{j+\frac{1}{2}} = \alpha_{j+\frac{1}{2}}\Delta v_{j+\frac{1}{2}} - L \left( \alpha_{j+\frac{1}{2}}\Delta v_{j+\frac{1}{2}}, \alpha_{j-\frac{1}{2}}\Delta v_{j-\frac{1}{2}} \right). \quad (10)$$

It is easily verified that the argument remains valid. These results may be summarized as

### Theorem 1 (Positivity Theorem)

Suppose that the discrete conservation law (5) contains a limited diffusive flux as defined by equations (9) or (10). Then the positivity condition (6), together with the properties (P1-P4) for limited averages, are sufficient to ensure satisfaction of the LED principle that a local maximum cannot increase and a local minimum cannot decrease.  $\square$

The new scheme will be referred to as the symmetric limited positive (SLIP) scheme. The construction benefits from the fact that the terms involving  $\phi(r^-)$  and  $\phi(r^+)$  reinforce the positivity of the coefficients whenever  $\phi$  is positive. Thus the only major restriction on  $L(u, v)$  is that it must be zero when  $u$  and  $v$  have opposite signs, or that  $\phi(r) = 0$  when  $r < 0$ . If  $\Delta v_{j+\frac{1}{2}}$  and  $\Delta v_{j-\frac{1}{2}}$  have opposite signs then there is an extremum at either  $j$  or  $j+1$ . In the case of an odd-even mode, however, they have the same sign, which is opposite to that of  $\Delta v_{j+\frac{1}{2}}$ , so that

they reinforce the damping in the same way that a simple central fourth difference formula would. At the crest of a shock, if the upstream flow is constant then  $\Delta v_{j-\frac{1}{2}} = 0$ , and thus  $\Delta v_{j+\frac{1}{2}}$  is prevented from canceling any part of  $\Delta v_{j+\frac{1}{2}}$  because it is limited by  $\Delta v_{j-\frac{1}{2}}$ .

A variety of limiters may be defined which meet the requirements of properties (P1-P4). Define

$$S(u, v) = \frac{1}{2} \{ \text{sign}(u) + \text{sign}(v) \}$$

so that

$$S(u, v) = \begin{cases} 1 & \text{if } u > 0 \text{ and } v > 0 \\ 0 & \text{if } u \text{ and } v \text{ have opposite sign} \\ -1 & \text{if } u < 0 \text{ and } v < 0 \end{cases}$$

Three limiters which are appropriate are the following well-known schemes:

1. Minmod:

$$L(u, v) = S(u, v) \min(|u|, |v|)$$

2. Van Leer:

$$L(u, v) = S(u, v) \frac{2|u||v|}{|u| + |v|}$$

3. Superbee:

$$L(u, v) = S(u, v) \max \{ \min(2|u|, |v|), \min(|u|, 2|v|) \}$$

These are special cases of the following more general formulas:

4.  $\alpha$ -mod:

$$L(u, v) = S(u, v) \frac{(1 + \alpha)|u||v|}{\max(|u|, |v|) + \alpha \min(|u|, |v|)}$$

5.  $\alpha$ - $\beta$ -mod:

$$L(u, v) = S(u, v) \frac{(1 + \alpha)|u|^{\frac{\beta+1}{2}}|v|^{\frac{\beta+1}{2}}}{\max(|u|^\beta, |v|^\beta) + \alpha \min(|u|^\beta, |v|^\beta)}$$

6.  $\alpha$ -bee:

$$L(u, v) = S(u, v) \max \{ \min(\alpha|u|, |v|), \min(|u|, \alpha|v|) \}$$

$\alpha$ -mod reduces to minmod when  $\alpha = 0$ , and to Van Leer when  $\alpha = 1$ .  $\alpha$ - $\beta$ -mod reduces to the geometric mean when  $\beta = 0$  and  $u$  and  $v$  have the same sign, and to  $\alpha$ -mod when  $\beta = 1$ .  $\alpha$ -bee reduces to minmod when  $\alpha = 1$  and to superbee when  $\alpha = 2$ . Another formulation is simply to limit the arithmetic mean by some multiple of the smaller of  $|u|$  and  $|v|$ :

7.  $\alpha$ -mean:

$$L(u, v) = S(u, v) \min \left( \frac{|u+v|}{2}, \alpha|u|, \alpha|v| \right)$$

## 2.4 SLIP schemes on multi-dimensional unstructured meshes

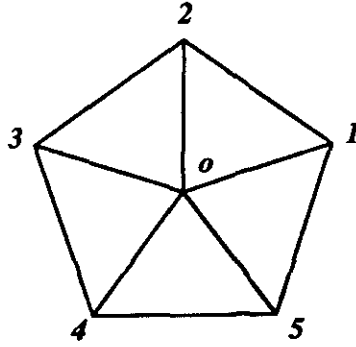


Figure 1: Cell Surrounding Vertex  $o$ .

Consider the discretization of the scalar conservation law (1) by a scheme in which  $v$  is represented at the vertices of a triangular mesh, as sketched in Figure 1. In a finite volume approximation (1) is written in integral form as

$$\frac{\partial}{\partial t} \int v \, ds + \oint f(v) \, dx - g(v) \, dy,$$

and this is approximated by trapezoidal integration around a polygon consisting of the triangles with a common vertex,  $o$ , say.

Thus (1) is discretized as

$$S \frac{dv_o}{dt} + \frac{1}{2} \sum_k \{ (f_k + f_{k-1})(y_k - y_{k-1}) - (g_k + g_{k-1})(x_k - x_{k-1}) \} = 0$$

where  $f_k = f(v_k)$ ,  $g_k = g(v_k)$ ,  $S$  is the area of the polygon, and  $k$  ranges over its vertices. This may be rearranged as

$$S \frac{dv_o}{dt} + \sum_k (f_k \Delta y_k - g_k \Delta x_k) = 0$$

where

$$\Delta x_k = \frac{1}{2}(x_{k+1} - x_{k-1}), \quad \Delta y_k = \frac{1}{2}(y_{k+1} - y_{k-1}).$$

Following, for example, References [8] and [11], this may now be reduced to a sum of differences over the edges  $ko$  by noting that  $\sum_k \Delta x_k = \sum_k \Delta y_k = 0$ . Consequently  $f_o$  and  $g_o$  may be added to give

$$S \frac{dv_o}{dt} + \sum \{ (f_k - f_o) \Delta y_k - (g_k - g_o) \Delta x_k \} = 0. \quad (11)$$

Define the coefficient  $a_{ko}$  as

$$a_{ko} = \begin{cases} \frac{(f_k - f_o) \Delta y_k - (g_k - g_o) \Delta x_k}{\Delta v_{ko}}, & v_k \neq v_o \\ \left( \frac{\partial f}{\partial v} \Delta y_k - \frac{\partial g}{\partial v} \Delta x_k \right) \Big|_{v=v_o}, & v_k = v_o \end{cases}$$

and

$$\Delta v_{ko} = v_k - v_o.$$

Then equation (11) reduces to

$$S \frac{dv_o}{dt} + \sum_k a_{ko} \Delta v_{ko} = 0.$$

To produce a scheme satisfying the sign condition (2), add a dissipative term on the right hand side of the form

$$\sum_k \alpha_{ko} \Delta v_{ko}, \quad (12)$$

where the coefficients  $\alpha_{ko}$  satisfy the condition

$$\alpha_{ko} \geq |a_{ko}|. \quad (13)$$

These simple schemes are far too dissipative. Antidiffusive terms may be added without violating the positivity condition (2) by the following generalization of the one-dimensional scheme. Considering again the scalar case, let  $l_{ko}$  be the vector connecting the edge  $ko$  and define the neighboring differences

$$\Delta^+ v_{ko} = l_{ko} \cdot \nabla^+ v, \quad \Delta^- v_{ko} = l_{ko} \cdot \nabla^- v,$$

where  $\nabla^\pm v$  are the gradients of  $v$  evaluated in the triangles out of which and into which  $l_{ko}$  points, as sketched in Figure 2. Arminjon and Dervieux have

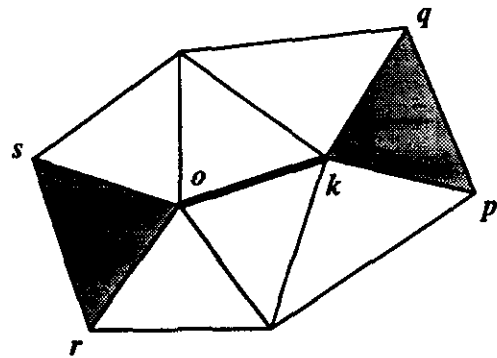


Figure 2: Edge  $ko$  and Adjacent Triangles.

used a similar definition [1].

It may now be verified that

$$\Delta^+ v_{ko} = \epsilon_{pk} (v_p - v_k) + \epsilon_{qk} (v_q - v_k)$$

and

$$\Delta^- v_{ko} = \epsilon_{or} (v_o - v_r) + \epsilon_{os} (v_o - v_s),$$

where the coefficients  $\epsilon_{pk}$ ,  $\epsilon_{qk}$ ,  $\epsilon_{or}$  and  $\epsilon_{os}$  are all non-negative. Now define the diffusive term for the edge  $ko$  as

$$d_{ko} = \alpha_{ko} \{ \Delta v_{ko} - L(\Delta^+ v_{ko}, \Delta^- v_{ko}) \}, \quad (14)$$

where  $L(u, v)$  is a limited average with the properties (P1-P4) that were defined in Section 2.3. In considering the sum of the terms at the vertex  $o$  write

$$L(\Delta^+ v_{ko}, \Delta^- v_{ko}) = \phi(r_{ko}^+) \Delta^- v_{ko},$$

where

$$r_{ko}^+ = \frac{\Delta^+ v_{ko}}{\Delta^- v_{ko}}.$$

Then, since the coefficients  $\epsilon_{or}$  and  $\epsilon_{os}$  are non-negative, and  $\phi(r_{ko}^+)$  is non-negative, the limited antidiffusive term in (14) produces a contribution from every edge which reinforces the positivity condition (2). Similarly, in considering the sum of the terms at  $k$  one writes

$$L(\Delta^+ v_{ko}, \Delta^- v_{ko}) = \phi(r_{ko}^-) \Delta^+ v_{ko},$$

where

$$r_{ko}^- = \frac{\Delta^- v_{ko}}{\Delta^+ v_{ko}},$$

and again the discrete equation receives a contribution with the right sign. One may therefore deduce the following result:

**Theorem 2 (Positivity Theorem for Unstructured Meshes)**

*Suppose that the discrete conservation law (11) is augmented by flux limited dissipation following equations (12) and (14). Then the positivity condition (13), together with the properties (P1-P4) for limited averages, are sufficient to ensure the LED property at every interior mesh point.  $\square$*

Note also that if this construction is applied to any linear function  $v$  then

$$\Delta v_{ko} = \Delta^+ v_{ko} = \Delta^- v_{ko},$$

with the consequence that the contribution of the diffusive terms is exactly zero. In the case of a smoothly varying function  $v$ , suppose that  $l_{ko} \cdot \nabla v \neq$

0 and the limiter is smooth in the neighborhood of  $r_{ko}^\pm = 1$ . Then substitution of a Taylor series expansion indicates that the magnitude of the diffusive flux will be of second order. At an extremum the antidiffusive term is cut off and the diffusive flux is of first order.

**2.5 Upstream limited positive (USLIP) schemes**

By adding the anti-diffusive correction purely from the upstream side one may derive a family of upstream limited positive (USLIP) schemes. Corresponding to the original SLIP scheme defined by equation (9), a USLIP scheme is obtained by setting

$$d_{j+\frac{1}{2}} = \alpha_{j+\frac{1}{2}} \left\{ \Delta v_{j+\frac{1}{2}} - L(\Delta v_{j+\frac{1}{2}}, \Delta v_{j-\frac{1}{2}}) \right\}$$

if  $\alpha_{j+\frac{1}{2}} > 0$ , or

$$d_{j+\frac{1}{2}} = \alpha_{j+\frac{1}{2}} \left\{ \Delta v_{j+\frac{1}{2}} - L(\Delta v_{j+\frac{1}{2}}, \Delta v_{j+\frac{3}{2}}) \right\}$$

if  $\alpha_{j+\frac{1}{2}} < 0$ . If  $\alpha_{j+\frac{1}{2}} = \frac{1}{2} |a_{j+\frac{1}{2}}|$  one recovers a standard high resolution upwind scheme in semi-discrete form. Consider the case that  $\alpha_{j+\frac{1}{2}} > 0$  and  $\alpha_{j-\frac{1}{2}} > 0$ . If one sets

$$r^+ = \frac{\Delta v_{j+\frac{1}{2}}}{\Delta v_{j-\frac{1}{2}}}, \quad r^- = \frac{\Delta v_{j-\frac{3}{2}}}{\Delta v_{j-\frac{1}{2}}},$$

the scheme reduces to

$$\Delta x \frac{dv_j}{dt} = -\frac{1}{2} \left\{ \phi(r^+) a_{j+\frac{1}{2}} + (2 - \phi(r^-)) a_{j-\frac{1}{2}} \right\} \Delta v_{j-\frac{1}{2}}.$$

To assure the correct sign to satisfy the LED criterion the flux limiter must now satisfy the additional constraint that  $\phi(r) \leq 2$ .

The USLIP construction can also be implemented on an unstructured mesh by taking

$$d_{ko} = |a_{ko}| \{ \Delta v_{ko} - L(\Delta v_{ko}, \Delta^- v_{ko}) \}$$

if  $a_{ko} > 0$  and

$$d_{ko} = |a_{ko}| \{ \Delta v_{ko} - L(\Delta v_{ko}, \Delta^+ v_{ko}) \}$$

if  $a_{ko} < 0$ . Let  $\sum^+$  and  $\sum^-$  denote sums over the edges meeting at the vertex  $o$  for which  $a_{ko} > 0$  and  $a_{ko} < 0$ . Define

$$r_{ko}^+ = \frac{\Delta v_{ko}}{\Delta v_{k_o^-}}, \quad r_{ko}^- = \frac{\Delta v_{k_o^+}}{\Delta v_{ko}}$$

Then

$$\Delta x \frac{dv_o}{dt} = - \sum^+ a_{k_o} \phi(r_{k_o}^+) \Delta^- v_{k_o} - \sum^- a_{k_o} (2 - \phi(r_{k_o}^-)) \Delta v_{k_o}$$

and substituting the formula for  $\Delta^- v_{k_o}$  the coefficient of every difference  $\Delta v_{k_o}$  is found to be non-negative, with the consequence that the scheme is LED.

## 2.6 General construction of higher order SLIP schemes

Schemes of any desired order of accuracy in regions where the solution does not contain extrema can be constructed by the following general procedure. Suppose that the scalar conservation law (1) is approximated in semi-discrete form by the low and high order schemes

$$\Delta x \frac{dv_j}{dt} + f_{L_{j+\frac{1}{2}}} - f_{L_{j-\frac{1}{2}}} = 0 \quad (15)$$

and

$$\Delta x \frac{dv_j}{dt} + f_{H_{j+\frac{1}{2}}} - f_{H_{j-\frac{1}{2}}} = 0 \quad (16)$$

where the low order scheme has positive coefficients and is local extremum diminishing (LED). Define an anti-diffusive flux as

$$A_{j+\frac{1}{2}} = f_{H_{j+\frac{1}{2}}} - f_{L_{j+\frac{1}{2}}},$$

and in order to define a limited corrective flux  $f_{C_{j+\frac{1}{2}}}$  let  $B_{j+\frac{1}{2}}$  be a bound determined from the local slopes as

$$B_{j+\frac{1}{2}} = \left| \min \text{mod} \left( \Delta v_{j+\frac{3}{2}}, \Delta v_{j+\frac{1}{2}}, \Delta v_{j-\frac{1}{2}} \right) \right|,$$

where  $\min \text{mod}(u, v, w) = 0$  if  $u, v,$  and  $w$  do not have the same sign, and otherwise

$$\min \text{mod}(u, v, w) = S \min(|u|, |v|, |w|),$$

where  $S$  is the sign of  $u, v,$  and  $w$ . Set

$$f_{C_{j+\frac{1}{2}}} = \text{sign}(A_{j+\frac{1}{2}}) \min \left( \left| A_{j+\frac{1}{2}} \right|, \beta_{j+\frac{1}{2}} B_{j+\frac{1}{2}} \right), \quad (17)$$

where  $\beta_{j+\frac{1}{2}} > 0$ . The SLIP scheme is now defined as

$$\Delta x \frac{dv_j}{dt} + h_{j+\frac{1}{2}} - h_{j-\frac{1}{2}} = 0, \quad (18)$$

where

$$h_{j+\frac{1}{2}} = f_{L_{j+\frac{1}{2}}} + f_{C_{j+\frac{1}{2}}}. \quad (19)$$

Thus, it reduces to the high order scheme when the limiters are not active. It is important that the limiter depends only on the magnitude of the local slopes, and not their sign, so that the correction can have either sign.

In order to prove that the general SLIP scheme is LED, note that the low order LED scheme can be written as

$$\Delta x \frac{dv_j}{dt} = c_{j+\frac{1}{2}}^+ \Delta v_{j+\frac{1}{2}} - c_{j-\frac{1}{2}}^- \Delta v_{j-\frac{1}{2}},$$

where  $c_{j+\frac{1}{2}}^+ \geq 0$  and  $c_{j-\frac{1}{2}}^- \geq 0$ . Now,

$$\min \left( \left| A_{j+\frac{1}{2}} \right|, \beta_{j+\frac{1}{2}} B_{j+\frac{1}{2}} \right) = \gamma_{j+\frac{1}{2}} B_{j+\frac{1}{2}}, \quad 0 \leq \gamma_{j+\frac{1}{2}} \leq \beta_{j+\frac{1}{2}}.$$

Also,

$$B_{j+\frac{1}{2}} = \phi_{j+\frac{1}{2}}^+ \Delta v_{j+\frac{3}{2}} = \phi_{j+\frac{1}{2}} \Delta v_{j+\frac{1}{2}} = \phi_{j+\frac{1}{2}}^- \Delta v_{j-\frac{1}{2}},$$

where

$$0 \leq \phi_{j+\frac{1}{2}}^+ \leq 1, \quad 0 \leq \phi_{j+\frac{1}{2}} \leq 1, \quad 0 \leq \phi_{j+\frac{1}{2}}^- \leq 1$$

since  $B_{j+\frac{1}{2}} = 0$  if  $v_{j+\frac{3}{2}}, v_{j+\frac{1}{2}},$  and  $v_{j-\frac{1}{2}}$  do not all have the same sign.

Define

$$s_{j+\frac{1}{2}} = \text{sign}(\Delta v_{j+\frac{1}{2}}), \quad s_{A_{j+\frac{1}{2}}} = \text{sign}(A_{j+\frac{1}{2}}).$$

Then, since  $B_{j+\frac{1}{2}} = B_{j-\frac{1}{2}} = 0$  unless  $s_{j+\frac{1}{2}} = s_{j-\frac{1}{2}} = 0$ ,

$$\begin{aligned} f_{C_{j-\frac{1}{2}}} - f_{C_{j+\frac{1}{2}}} = & \\ & + \frac{1}{2} \left| s_{j+\frac{1}{2}} + s_{A_{j-\frac{1}{2}}} \right| \gamma_{j-\frac{1}{2}} \phi_{j-\frac{1}{2}}^+ \Delta v_{j+\frac{1}{2}} \\ & - \frac{1}{2} \left| s_{j-\frac{1}{2}} - s_{A_{j-\frac{1}{2}}} \right| \gamma_{j-\frac{1}{2}} \phi_{j-\frac{1}{2}} \Delta v_{j-\frac{1}{2}} \\ & + \frac{1}{2} \left| s_{j+\frac{1}{2}} - s_{A_{j+\frac{1}{2}}} \right| \gamma_{j+\frac{1}{2}} \phi_{j+\frac{1}{2}} \Delta v_{j+\frac{1}{2}} \\ & - \frac{1}{2} \left| s_{j-\frac{1}{2}} + s_{A_{j+\frac{1}{2}}} \right| \gamma_{j+\frac{1}{2}} \phi_{j+\frac{1}{2}}^- \Delta v_{j-\frac{1}{2}} \end{aligned}$$

so that the correction reinforces the positivity of  $c_{j+\frac{1}{2}}^+$  and  $c_{j-\frac{1}{2}}^-$ . This provides the proof of

### Theorem 3 (Positivity of the General SLIP Scheme)

The semi-discrete scheme defined by equations (17-19) is LED if the low order scheme (15) is LED.

□

The key idea in this proof is that the correction  $A_{j+\frac{1}{2}}$  may be associated with either  $\Delta v_{j-\frac{1}{2}}$  or  $\Delta v_{j+\frac{1}{2}}$  depending on whether it has the same or the opposite sign as  $\Delta v_{j-\frac{1}{2}}$  and  $\Delta v_{j+\frac{1}{2}}$ .

The idea of blending high and low order schemes to produce a limited anti-diffusive correction is similar to that used in Zalesak's generalization of flux corrected transport (FCT) [24]. With FCT the anti-diffusion is introduced in a separate corrector stage, whereas in the present scheme it is integrated in the construction of the numerical flux. This brings it within the framework of a general theory of LED schemes, and facilitate its extension to treat systems of equations by the introduction of flux splitting procedures.

As an example of the general SLIP construction suppose that the numerical flux has the form

$$h_{j+\frac{1}{2}} = \frac{1}{2}(f_{j+1} + f_j) - d_{j+\frac{1}{2}},$$

where for the low order scheme

$$d_{j+\frac{1}{2}} = \alpha_{j+\frac{1}{2}} \Delta v_{j+\frac{1}{2}}, \quad \alpha_{j+\frac{1}{2}} \geq \frac{1}{2} |a_{j+\frac{1}{2}}|,$$

and for the high order scheme

$$d_{j+\frac{1}{2}} = \alpha_{j+\frac{1}{2}} \left( \Delta v_{j+\frac{1}{2}} - \frac{1}{2} \Delta v_{j+\frac{3}{2}} - \frac{1}{2} \Delta v_{j-\frac{1}{2}} \right).$$

These are just the diffusive fluxes which are used in the switched JST scheme described in Section 2.2. The anti-diffusive flux in the SLIP scheme is now

$$A_{j+\frac{1}{2}} = \frac{1}{2} \alpha_{j+\frac{1}{2}} \left( \Delta v_{j+\frac{3}{2}} + \Delta v_{j-\frac{1}{2}} \right).$$

In this case the bound  $B_{j+\frac{1}{2}}$  need only depend on the smaller of  $|\Delta v_{j+\frac{3}{2}}|$  and  $|\Delta v_{j-\frac{1}{2}}|$ , provided that  $\Delta v_{j+\frac{3}{2}}$  and  $\Delta v_{j-\frac{1}{2}}$  have the same sign, leading to the first SLIP scheme with  $\alpha$ -mean as the limiter. Here the SLIP construction provides an alternative switching procedure to the sensor in the JST scheme, such that the LED property is enforced.

To construct a sequence of successively higher order SLIP schemes one may start by constructing a second order scheme SLIP<sub>2</sub>, say by taking

$$\begin{aligned} f_{L_{j+\frac{1}{2}}}^{(1)} &= \frac{1}{2}(f_{j+1} + f_j) - \alpha_{j+\frac{1}{2}} \Delta v_{j+\frac{1}{2}} \\ f_{H_{j+\frac{1}{2}}}^{(1)} &= \frac{1}{2}(f_{j+1} + f_j) \\ &\quad + \alpha_{j+\frac{1}{2}} \left( \Delta v_{j+\frac{3}{2}} - 2\Delta v_{j+\frac{1}{2}} + \Delta v_{j-\frac{1}{2}} \right) \\ A_{j+\frac{1}{2}}^{(1)} &= f_{H_{j+\frac{1}{2}}}^{(1)} - f_{L_{j+\frac{1}{2}}}^{(1)} \\ h_{j+\frac{1}{2}}^{(1)} &= f_{L_{j+\frac{1}{2}}}^{(1)} \\ &\quad + \text{sign} \left( A_{j+\frac{1}{2}}^{(1)} \right) \min \left( |A_{j+\frac{1}{2}}^{(1)}|, \beta_{j+\frac{1}{2}} B_{j+\frac{1}{2}} \right) \end{aligned}$$

Then one may repeat the procedure, taking

$$\begin{aligned} f_{L_{j+\frac{1}{2}}}^{(2)} &= h_{j+\frac{1}{2}}^{(1)} \\ f_{H_{j+\frac{1}{2}}}^{(2)} &= \frac{1}{2}(f_{j+1} + f_j) - \frac{1}{12} \left( \Delta f_{j+\frac{3}{2}} - \Delta f_{j-\frac{1}{2}} \right) \\ &\quad - \frac{1}{6} \alpha_{j+\frac{1}{2}} \left( \Delta v_{j+\frac{3}{2}} - 4\Delta v_{j+\frac{1}{2}} + 6\Delta v_{j+\frac{1}{2}} - 4\Delta v_{j-\frac{1}{2}} + \Delta v_{j-\frac{3}{2}} \right), \end{aligned}$$

where

$$\Delta f_{j+\frac{1}{2}} = \Delta f_{j+1} - \Delta f_j,$$

and

$$\begin{aligned} A_{j+\frac{1}{2}}^{(2)} &= f_{H_{j+\frac{1}{2}}}^{(2)} - f_{L_{j+\frac{1}{2}}}^{(2)} \\ h_{j+\frac{1}{2}}^{(2)} &= f_{L_{j+\frac{1}{2}}}^{(2)} \text{sign} \left( A_{j+\frac{1}{2}}^{(2)} \right) \min \left( |A_{j+\frac{1}{2}}^{(2)}|, \beta_{j+\frac{1}{2}} B_{j+\frac{1}{2}} \right). \end{aligned}$$

The resulting scheme, which may be conveniently labelled SLIP<sub>4</sub>, is fourth order accurate when the limiters are inactive. The procedure may be then be iterated. The correction  $f_{H_{j+\frac{1}{2}}}^{(2)} - f_{L_{j+\frac{1}{2}}}^{(2)}$  is of order  $\Delta x^2$ , and subsequent corrections are of correspondingly higher order. Thus they are progressively less likely to be limited by the bound  $B_{j+\frac{1}{2}}$ .

## 2.7 General SLIP scheme on unstructured meshes

The general SLIP construction may also be implemented on unstructured meshes. With the notation of Figure 3, let  $f_{L_{ko}}$  and  $f_{H_{ko}}$  be low and high order

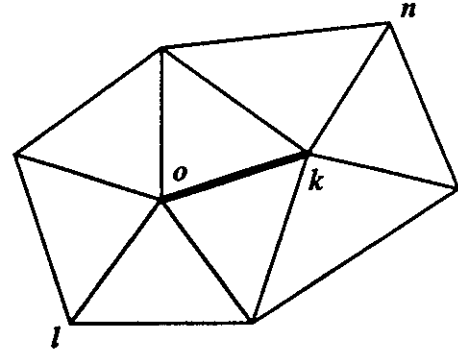


Figure 3: Edge  $ko$  and Adjacent Edges.

fluxes along the edge  $ko$ . Define the anti-diffusive flux along this edge as

$$A_{ko} = f_{H_{ko}} - f_{L_{ko}} \quad (20)$$

and the limited corrective flux as

$$f_{C_{ko}} = \text{sign}(A_{ko}) \min(|A_{ko}|, \beta_{ko} B_{ko}), \quad (21)$$

where  $\beta_{ko} > 0$  and  $B_{ko}$  is a bound determined by the local slopes. In order to define  $B_{ko}$  let  $l$  and  $n$  be any vertices neighboring  $k$  and  $o$  such that

$$\text{sign}(\Delta v_{nk}) = \text{sign}(\Delta v_{ko}), \quad \text{sign}(\Delta v_{ol}) = \text{sign}(\Delta v_{ko}).$$

If there is no such vertex  $n$  then  $k$  is a local extremum, and if there is no such vertex  $l$  then  $o$  is a local extremum. In either case set  $B_{ko} = 0$ . Otherwise set

$$B_{ko} = \min(|\Delta v_{nk}|, |\Delta v_{ko}|, |\Delta v_{ol}|). \quad (22)$$

The flux along the edge  $ko$  for the SLIP scheme is now defined as

$$f_{ko} = f_{L_{ko}} + f_{C_{ko}}.$$

It may be verified that the scheme can be expressed in terms of differences between the vertex  $o$  and its nearest neighbors with non-negative coefficients by adapting the one-dimensional derivation of the last section in the same way that the one-dimensional derivation of Section 2.3 was adapted to the unstructured mesh in Section 2.4. This result may be stated as

#### Theorem 4 (Positivity of the General SLIP Scheme on Unstructured Meshes)

If the discrete conservation law (11) is augmented by the diffusive flux  $f_{L_{ko}}$  and  $f_{C_{ko}}$  defined by equations (20–22), then the scheme is LED at every interior point.  $\square$

The construction requires the identification of any three edges  $lo$ ,  $ok$  and  $kn$  along which the solution is monotonically increasing or decreasing. If  $\Delta v_{ko} > 0$  one could search for vertices  $l$  and  $n$  which maximize  $\Delta v_{nk}$  and  $\Delta v_{ol}$ , but since the number of edges meeting at a given vertex can be very large, this procedure could be expensive, and one might prefer to apply the test to the edges  $nk$  and  $ol$  most nearly aligned with the edge  $ko$ .

### 2.8 Fully discrete LED schemes

When a discrete time stepping scheme is introduced to produce a fully discrete scheme, let a superscript  $n$  denote the time level. A convenient interpretation of the LED principle is now to require that the change  $\delta v_j = v_j^{n+1} - v_j^n$  should be limited so that  $v_j^{n+1}$  remains within thresholds set by the

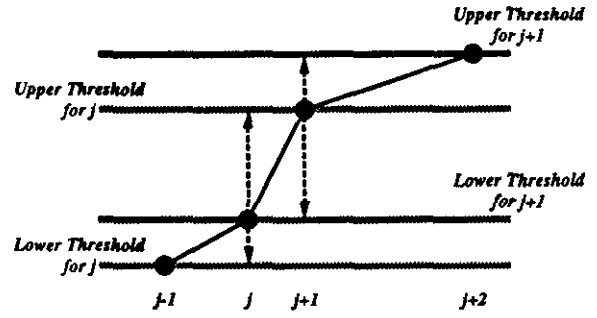


Figure 4: Thresholds for a Fully Discrete LED Scheme.

values  $v_{j-1}^n$  and  $v_{j+1}^n$ . One must consider the interaction of the flux  $h_{j+\frac{1}{2}}$  with both the changes  $\delta v_j$  and  $\delta v_{j+1}$ .

If one takes the simplest case of a forward Euler scheme

$$v_j^{n+1} = v_j^n - \frac{\Delta t}{\Delta x} (h_{j+\frac{1}{2}} - h_{j-\frac{1}{2}})$$

both the SLIP and the USLIP schemes remain valid but this constraint leads to a limit on the time step  $\Delta t$ . Let the flux limiting function  $\phi(r)$  satisfy the bound  $\phi(r) \leq \phi_{\max}$ . Then the limit on  $\Delta t$  becomes smaller as  $\phi_{\max}$  becomes larger. Similarly in the case of the general construction of Sections 2.6 and 2.7 the limit on  $\Delta t$  becomes smaller as the parameter  $\beta$  is increased. If the scheme is LED it is also stable in the  $L_\infty$  norm. Thus if  $\Delta t$  satisfies the LED restriction, the forward Euler scheme is stable. Given a forward Euler scheme that satisfies the positivity conditions, Shu has shown how to construct higher order multistage time stepping schemes which preserve these conditions under an appropriate restriction of the time step [18].

## 3 Systems of conservation laws

### 3.1 Flux splitting

Steger and Warming [20] first showed how to generalize the concept of upwinding to the system of conservation laws

$$\frac{\partial w}{\partial t} + \frac{\partial}{\partial x} f(w) = 0 \quad (23)$$

by the concept of flux splitting. Suppose that the flux is split as  $f = f^+ + f^-$  where  $\frac{\partial f^+}{\partial w}$  and  $\frac{\partial f^-}{\partial w}$  have positive and negative eigenvalues. Then the

first order upwind scheme is produced by taking the numerical flux to be

$$h_{j+\frac{1}{2}} = f_j^+ + f_{j+1}^-.$$

This can be expressed in viscosity form as

$$\begin{aligned} h_{j+\frac{1}{2}} &= +\frac{1}{2}(f_{j+1}^+ + f_j^+) - \frac{1}{2}(f_{j+1}^+ - f_j^+) \\ &\quad + \frac{1}{2}(f_{j+1}^- + f_j^-) + \frac{1}{2}(f_{j+1}^- - f_j^-) \\ &= \frac{1}{2}(f_{j+1} + f_j) - d_{j+\frac{1}{2}}, \end{aligned}$$

where the diffusive flux is

$$d_{j+\frac{1}{2}} = \frac{1}{2}\Delta(f^+ - f^-)_{j+\frac{1}{2}}. \quad (24)$$

Roe derived the alternative formulation of flux difference splitting [17] by distributing the corrections due to the flux difference in each interval upwind and downwind to obtain

$$\Delta x \frac{dw_j}{dt} + (f_{j+1} - f_j)^- + (f_j - f_{j-1})^+ = 0,$$

where now the flux difference  $f_{j+1} - f_j$  is split. The corresponding diffusive flux is

$$d_{j+\frac{1}{2}} = \frac{1}{2}(\Delta f_{j+\frac{1}{2}}^+ - \Delta f_{j+\frac{1}{2}}^-).$$

Following Roe's derivation, let  $A_{j+\frac{1}{2}}$  be a mean value Jacobian matrix exactly satisfying the condition

$$f_{j+1} - f_j = A_{j+\frac{1}{2}}(w_{j+1} - w_j).$$

Then a splitting according to characteristic fields is obtained by decomposing  $A_{j+\frac{1}{2}}$  as

$$A_{j+\frac{1}{2}} = T\Lambda T^{-1},$$

where the columns of  $T$  are the eigenvectors of  $A_{j+\frac{1}{2}}$ , and  $\Lambda$  is a diagonal matrix of the eigenvalues. Then

$$\Delta f_{j+\frac{1}{2}}^\pm = T\Lambda^\pm T^{-1}\Delta w_{j+\frac{1}{2}}.$$

Now the corresponding diffusive flux is

$$\frac{1}{2}|A_{j+\frac{1}{2}}|(w_{j+1} - w_j),$$

where

$$|A_{j+\frac{1}{2}}| = T|\Lambda|T^{-1}$$

and  $|\Lambda|$  is the diagonal matrix containing the absolute values of the eigenvalues.

Simple stable schemes can be produced by the splitting

$$(f_{j+1} - f_j)^\pm = \frac{1}{2}(f_{j+1} - f_j) \pm \alpha_{j+\frac{1}{2}}(w_{j+1} - w_j),$$

which satisfies the positivity condition on the eigenvalues if  $\alpha_{j+\frac{1}{2}} > \frac{1}{2} \max |\lambda(A_{j+\frac{1}{2}})|$  and corresponds to the scalar diffusive flux

$$d_{j+\frac{1}{2}} = \alpha_{j+\frac{1}{2}}\Delta w_{j+\frac{1}{2}}. \quad (25)$$

Characteristic splitting has the advantage that it allows a discrete shock structure with a single interior point. The simple scalar diffusive flux (25) is computationally inexpensive, and combined with the high resolution switched scheme captures shock waves about three interior points.

### 3.2 Construction of convective upwind and split pressure (CUSP) schemes

Discrete schemes should be designed to provide high accuracy in smooth regions in combination with oscillation-free shocks at the lowest possible computational cost. This in turn requires both economy in the formulation, and in the case of steady state calculations, a rapidly convergent iterative scheme. The convective upwind and split pressure (CUSP) scheme described below meets these requirements, while providing excellent shock resolution at high Mach numbers. When very sharp resolution of weak shocks is required, the results can be improved by characteristic splitting with matrix diffusion using Roe averaging.

Consider the one-dimensional equations for gas dynamics. In this case the solution and flux vectors appearing in equation (23) are

$$w = \begin{pmatrix} \rho \\ \rho u \\ \rho E \end{pmatrix}, \quad f = \begin{pmatrix} \rho u \\ \rho u^2 + p \\ \rho u H \end{pmatrix},$$

where  $\rho$  is the density,  $u$  is the velocity,  $E$  is the total energy,  $p$  is the pressure, and  $H$  is the stagnation enthalpy. If  $\gamma$  is the ratio of specific heats and  $c$  is the speed of sound

$$p = (\gamma - 1)\rho \left( E - \frac{u^2}{2} \right)$$

$$c^2 = \frac{\gamma p}{\rho}$$

$$H = E + \frac{p}{\rho} = \frac{c^2}{\gamma - 1} + \frac{u^2}{2}.$$

In a steady flow  $H$  is constant. This remains true for the discrete scheme only if the diffusion is constructed so that it is compatible with this condition.

The eigenvalues of the Jacobian matrix  $A = \frac{\partial f}{\partial w}$  are  $u$ ,  $u+c$ , and  $u-c$ . If  $u > 0$  and the flow is locally supersonic ( $M = \frac{u}{c} > 1$ ), all the eigenvalues are positive, and simple upwinding is thus a natural choice for diffusion in supersonic flow. It is convenient to consider the convective and pressure fluxes

$$f_c = u \begin{pmatrix} \rho \\ \rho u \\ \rho H \end{pmatrix} = u w_c, \quad f_p = \begin{pmatrix} 0 \\ p \\ 0 \end{pmatrix}$$

separately. Upwinding of the convective flux is achieved by

$$d_{c_{j+\frac{1}{2}}} = |u_{j+\frac{1}{2}}| \Delta w_{c_{j+\frac{1}{2}}} = |M| c_{j+\frac{1}{2}} \Delta w_{c_{j+\frac{1}{2}}},$$

where  $M$  is the local Mach number attributed to the interval. Upwinding of the pressure is achieved by

$$d_{p_{j+\frac{1}{2}}} = \text{sign}(M) \begin{pmatrix} 0 \\ \Delta p_{j+\frac{1}{2}} \\ 0 \end{pmatrix}.$$

Full upwinding of both  $f_c$  and  $f_p$  is incompatible with stability in subsonic flow, since pressure waves with the speed  $u - c$  would be traveling backwards, and the discrete scheme would not have a proper zone of dependence. Since the eigenvalues of  $\frac{\partial f_c}{\partial w}$  are  $u$ ,  $u$  and  $\gamma u$ , while those of  $\frac{\partial f_p}{\partial w}$  are  $0$ ,  $0$  and  $-(\gamma - 1)u$ , a split with

$$f^+ = f_c, \quad f^- = f_p$$

leads to a stable scheme, used by Denton [4], in which downwind differencing is used for the pressure.

This scheme does not reflect the true zone of dependence in supersonic flow. Thus one may seek a scheme with

$$\begin{aligned} d_{c_{j+\frac{1}{2}}} &= f_1(M) c_{j+\frac{1}{2}} \Delta w_{c_{j+\frac{1}{2}}} \\ d_{p_{j+\frac{1}{2}}} &= f_2(M) \begin{pmatrix} 0 \\ \Delta p_{j+\frac{1}{2}} \\ 0 \end{pmatrix}, \end{aligned}$$

where  $f_1(M)$  and  $f_2(M)$  are blending functions with the asymptotic behavior  $f_1(M) \rightarrow |M|$  and  $f_2(M) \rightarrow \text{sign}(M)$  for  $|M| > 1$ . Also the convective diffusion should remain positive when  $M = 0$ , while the pressure diffusion must be antisymmetric with respect to  $M$ . A simple choice is to take  $f_1(M) = |M|$  and  $f_2(M) = \text{sign}(M)$  for  $|M| > 1$ , and to introduce blending polynomials in  $M$  for

$|M| < 1$  which merge smoothly into the supersonic segments. A quartic formula

$$f_1(M) = a_0 + a_2 M^2 + a_4 M^4, \quad |M| < 1$$

preserves continuity of  $f_1$  and  $\frac{df_1}{dM}$  at  $|M| = 1$  if

$$a_2 = \frac{3}{2} - 2a_0, \quad a_4 = a_0 - \frac{1}{2}.$$

Then  $a_0$  controls the diffusion at  $M = 0$ . For transonic flow calculations a good choice is  $a_0 = \frac{1}{4}$ , while for very high speed flows it may be increased to  $\frac{1}{2}$ . A suitable blending formula for the pressure diffusion is

$$f_2(M) = \frac{1}{2} M (3 - M^2), \quad |M| < 1.$$

The diffusion corresponding to the convective terms is identical to the scalar diffusion of Jameson, Schmidt and Turkel [12], with a modification of the scaling, while the pressure term is the minimum modification needed to produce perfect upwinding in the supersonic zone. The scheme retains the property of the original scheme that it is compatible with constant stagnation enthalpy in steady flow. If one derives the viscosity corresponding to the flux splitting recently proposed by Liou and Steffen [15], following equation (24), one finds that their scheme produces first order diffusion with a similar general form, and the present scheme may thus be regarded as a construction of artificial viscosity approximately equivalent to Liou-Steffen splitting.

### 3.3 Multi-dimensional systems

Schemes for structured meshes are conveniently constructed treating each mesh direction separately in a manner similar to the one-dimensional case. For unstructured meshes, the three-dimensional conservation law

$$\frac{\partial v}{\partial t} + \frac{\partial}{\partial x} f(v) + \frac{\partial}{\partial y} g(v) + \frac{\partial}{\partial z} h(v) = 0 \quad (26)$$

can be treated in a manner similar to the scalar case by first expressing the convective flux balance as a sum of differences along edges. Consider the set of tetrahedrons containing a common edge. Then one may associate with that edge a vector area  $S$  which is one-third the sum of the areas of the set of faces which form one of two opposing umbrellas around the edge. With a notation similar to that of Figure 1 the convective flux balance corresponding to

equation (26) at an interior mesh point may be written as

$$V \frac{dw_o}{dt} + \sum_k (\mathbf{F}_k - \mathbf{F}_o) \cdot \mathbf{S}_{ko} = 0, \quad (27)$$

where the columns of  $\mathbf{F}$  are the flux vectors  $f$ ,  $g$  and  $h$ , and  $V$  is the volume of the polyhedron formed by the union of all the tetrahedrons with the common vertex  $o$ . Here  $\mathbf{F}_o$  may be added or subtracted since  $\sum_k \mathbf{S}_{ko} = \mathbf{0}$ . Diffusion may now be added along the edges in exactly the same way as before. When the convective flux balance is evaluated, it is more convenient to use the sum  $\sum_k (\mathbf{F}_k + \mathbf{F}_o) \cdot \mathbf{S}_{ko}$ , so that the convective flux along each edge needs to be calculated only once in a loop over the edges and appropriately accumulated at nodes  $k$  and  $o$ .

The SLIP scheme can now be formulated with the aid of Roe's construction [17]. Let  $A_{ko}$  be a matrix such that

$$A_{ko} (w_k - w_o) = (\mathbf{F}_k - \mathbf{F}_o) \cdot \mathbf{S}_{ko}.$$

Suppose that  $A_{ko}$  is decomposed as  $TAT^{-1}$  where the columns  $t_j$  of  $T$  are the eigenvectors of  $A_{ko}$ . Then the difference  $\Delta w = w_k - w_o$  is expressed as a sum  $\sum_j \alpha_j t_j$  of the eigenvectors, where the coefficients  $\alpha_j = (T^{-1} \Delta w)_j$  represent the characteristic variables, and the diffusive term along the edge  $ko$  is constructed as

$$|A_{ko}| \Delta w = T |A| T^{-1} \Delta w.$$

In order to construct a higher order scheme, an anti-diffusive flux may then be calculated by applying the limited averaging procedure as in equation (14) to each characteristic variable separately.

At boundary points equations (11) or (27) need to be augmented by additional fluxes through the boundary edges or faces. The first order diffusive flux  $\alpha_{ko} \Delta v_{ko}$  may be offset by subtracting an anti-diffusive flux evaluated from the interior, taking a limited average with  $\Delta v_{ko}$ .

## 4 Convergence acceleration for steady state calculations

### 4.1 Time stepping schemes

The discretization of the spatial derivatives reduces the partial differential equation to a semi-discrete

equation which may be written in the form

$$\frac{dw}{dt} + R(w) = 0, \quad (28)$$

where  $w$  is the vector of flow variables at the mesh points, and  $R(w)$  is the vector of the residuals, consisting of the flux balances augmented by the diffusive terms. In the case of a steady state calculation the details of the transient solution are immaterial, and the time stepping scheme may be designed solely to maximize the rate of convergence.

If an explicit scheme is used, the permissible time step for stability may be so small that a very large number of time steps are needed to reach a steady state. This can be alleviated by using time steps of varying size in different locations, which are adjusted so that they are always close to the local stability limit. If the mesh interval increases with the distance from the body, the time step will also increase, producing an effect comparable to that of an increasing wave speed. Convergence to a steady state can be further accelerated by the use of a multigrid procedure of the type described below. With the aid of these measures explicit multistage schemes have proved extremely effective. Implicit schemes allow much larger time steps, but the work required in each time step may become excessively large, especially in three-dimensional calculations. In fact, it is suggested in the next section that a good way to construct efficient implicit schemes for calculating unsteady flows is to use an explicit multigrid scheme to solve the equations in each time step.

If one reduces the linear model problem corresponding to (28) to an ordinary differential equation by substituting a Fourier mode  $\hat{w} = e^{ipx}$ , the resulting Fourier symbol has an imaginary part proportional to the wave speed, and a negative real part proportional to the diffusion. Thus the time stepping scheme should have a stability region which contains a substantial interval of the negative real axis, as well as an interval along the imaginary axis. To achieve this it pays to treat the convective and dissipative terms in a distinct fashion. Thus the residual is split as

$$R(w) = Q(w) + D(w),$$

where  $Q(w)$  is the convective part and  $D(w)$  the dissipative part. Denote the time level  $n\Delta t$  by a superscript  $n$ . Then the multistage time stepping

scheme is formulated as

$$\begin{aligned} w^{(n+1,0)} &= w^n \\ &\dots \\ w^{(n+1,k)} &= w^n - \alpha_k \Delta t \left( Q^{(k-1)} + D^{(k-1)} \right) \\ &\dots \\ w^{n+1} &= w^{(n+1,m)}, \end{aligned}$$

where the superscript  $k$  denotes the  $k$ -th stage,  $\alpha_m = 1$ , and

$$\begin{aligned} Q^{(0)} &= Q(w^n), \quad D^{(0)} = D(w^n) \\ &\dots \\ Q^{(k)} &= Q(w^{(n+1,k)}) \\ D^{(k)} &= \beta_k D(w^{(n+1,k)}) + (1 - \beta_k) D^{(k-1)}. \end{aligned}$$

The coefficients  $\alpha_k$  are chosen to maximize the stability interval along the imaginary axis, and the coefficients  $\beta_k$  are chosen to increase the stability interval along the negative real axis.

Two schemes which have been found to be particularly effective are tabulated below. The first is a four-stage scheme with two evaluations of dissipation. Its coefficients are

$$\begin{aligned} \alpha_1 &= \frac{1}{3} & \beta_1 &= 1 \\ \alpha_2 &= \frac{4}{15} & \beta_2 &= \frac{1}{2} \\ \alpha_3 &= \frac{5}{9} & \beta_3 &= 0 \\ \alpha_4 &= 1 & \beta_4 &= 0 \end{aligned}$$

The second is a five-stage scheme with three evaluations of dissipation. Its coefficients are

$$\begin{aligned} \alpha_1 &= \frac{1}{4} & \beta_1 &= 1 \\ \alpha_2 &= \frac{1}{6} & \beta_2 &= 0 \\ \alpha_3 &= \frac{3}{8} & \beta_3 &= 0.56 \\ \alpha_4 &= \frac{1}{2} & \beta_4 &= 0 \\ \alpha_5 &= 1 & \beta_5 &= 0.44 \end{aligned}$$

## 4.2 Multigrid

The multigrid scheme is a full approximation scheme defined as follows [6, 8]. Denote the grids by a subscript  $k$ . Start with a time step on the finest grid  $k = 1$ . Transfer the solution from a given grid to a coarser grid by a transfer operator  $P_{k,k-1}$ , so that the initial state on grid  $k$  is

$$w_k^{(0)} = P_{k,k-1} w_{k-1}.$$

Then on grid  $k$  the multistage time stepping scheme is reformulated as

$$w_k^{(q+1)} = w_k^{(0)} - \alpha_n \Delta t \left( R_k^{(q)} + G_k \right),$$

where the residual  $R_k^{(q)}$  is evaluated from current and previous values as above, and the forcing function  $G_k$  is defined as the difference between the aggregated residuals transferred from grid  $k-1$  and the residual recalculated on grid  $k$ . Thus

$$G_k = Q_{k,k-1} R(w_{k-1}) - R(w_k^{(0)}),$$

where  $Q_{k,k-1}$  is another transfer operator. On the first stage the forcing term  $G_k$  simply replaces the coarse grid residual by the aggregated fine grid residuals. The accumulated correction on a coarser grid is transferred to the next higher grid by an interpolation operator  $I_{k-1,k}$  so that the solution on grid  $k-1$  is updated by the formula

$$w_{k-1}^{new} = w_{k-1} + I_{k-1,k} \left( w_k - w_k^{(0)} \right).$$

The whole set of grids is traversed in a  $W$ -cycle in which time steps are only performed when moving down the cycle.

## 5 Numerical results

In extensive numerical tests, schemes using the CUSP diffusive flux and the characteristic split flux with Roe averaging have both been found to give high resolution of shock waves. Figures 5-9 display the results of multigrid calculations using the CUSP scheme with adaptive diffusion using the JST switch as defined by equations (8). The switch is applied to the pressure. With this construction the role of the high order diffusion is to provide global damping of oscillatory modes which would otherwise inhibit convergence to a steady state, while the role of the first order diffusion is to control oscillations near discontinuities. Numerical experiments with multigrid acceleration confirm that the rate of convergence to a steady state is essentially the same when the first order diffusion is eliminated, but large pre- and post-shock oscillations appear in the solution. On the other hand the multigrid scheme will not converge if the global diffusion is eliminated.

Figures 5-7 show transonic solutions for three different airfoils, calculated on a  $160 \times 32$  mesh, and each of which is essentially converged in 12 multigrid cycles. The work in each cycle is about equal to two explicit time steps on the fine grid. It may be noted also that the computed drag coefficient of the Korn airfoil at the shock-free design point is zero to

four digits. The drag coefficient is also computed to be zero to four digits for subsonic flows over a variety of airfoils with lift coefficients in the range up to 1.0. Very little change is observed between solutions calculated on  $80 \times 16$  and  $160 \times 32$  meshes, providing a further confirmation of accuracy.

The CUSP scheme produces very sharp shock waves in hypersonic flow, provided that care is taken to define the cell interface Mach number as the Mach number on the downwind side, so that downwind terms are perfectly canceled in supersonic flow. This is illustrated in Figures 8 and 9, which show the flow past a semicircular blunt body at Mach 8 and 20. It can be seen that quite rapid convergence, at a rate of the order of 0.9, continues to be obtained with the multigrid scheme in hypersonic flow.

Shock waves in transonic flow are less sharply resolved, but discrete shock waves with 2 or 3 interior points are obtained if the diffusion is scaled to a value somewhat less than that corresponding to full upwinding. Another way to achieve this is to use blending functions with the same asymptotic values for large Mach numbers, but smaller values when  $M = 1$ . One choice is

$$f_1(M) = \sqrt{\frac{1}{4} + M^2} \frac{\frac{1}{4} + M^2}{1 + M^2}, \quad f_2(M) = \frac{M}{\sqrt{1 + M^2}}.$$

The SLIP construction can be applied in conjunction with the CUSP diffusive flux, but limiters should not be applied indiscriminately to solution variables in regions where new extrema should be permitted to appear. Studies which are currently underway indicate, however, that they may be useful in improving the resolution of boundary layers [23] in the results presented here the SLIP construction is used in conjunction with characteristic splitting and Roe averaging, which may also be regarded as the use of matrix diffusion [21].

To verify that the SLIP construction presents oscillations in both steady and unsteady flows, Figure 10 shows the results of a shock tube calculation for the Sod problem [19]. This calculation was performed with the fourth order SLIP scheme formulated in Section 2.6. In the one-dimensional case single stage time stepping schemes of second or higher order similar to the Lax-Wendroff scheme can be derived at little cost in complexity by the successive substitution of space derivatives for time derivatives. Here, since the purpose was to verify the LED prop-

erty of the SLIP scheme, a simple forward Euler time stepping scheme was used with a time step corresponding to a Courant number of  $\frac{1}{3}$ . The computed results are superposed on the exact solution. The shock wave and expansion are very well resolved. The contact discontinuity is less sharply resolved, as is to be expected because of the absence of a natural compressive effect at a contact discontinuity.

Figures 11-14 present results of two dimensional transonic flow calculations with characteristic splitting, which confirm that stationary shock waves are very sharply resolved. Discrete shock waves with just one interior point are obtained when flux limited dissipation is used with the SLIP formulation, following equation (9). The choice of limiter can significantly affect the accuracy. If the limiter is too stringent the lift is noticeably underpredicted even on a  $320 \times 64$  mesh. For example, if one uses  $\alpha$ -mean with  $\alpha = 1$  the lift coefficient for the RAE 2822 airfoil at Mach 0.75 and  $3^\circ$  angle of attack is calculated on a  $320 \times 64$  mesh to be 1.092, whereas with  $\alpha = 2$  it is calculated to be 1.121. When the limiter is relaxed, on the other hand, it becomes progressively more difficult to achieve convergence to a steady state, and there is a tendency for convergence to stop at an error threshold in the region of  $10^4$ . The switched scheme can produce equally perfect shocks in steady flow when it is combined with characteristic splitting, provided that the shocks are not too weak. When multigrid acceleration is introduced it also generally converges more rapidly to a steady state. Thus it may be preferred for steady state calculations, while flux limited dissipation may be needed for perfect oscillation control in the calculation of unsteady flows.

Figures 11-12 show the results of multigrid calculations on a  $320 \times 64$  mesh for the RAE 2822 airfoil at Mach 0.75 and  $3^\circ$  angle of attack calculated with the switched scheme, and with the SLIP scheme using  $\alpha$ -mean with  $\alpha = 1.5$ . Figures 13-14 show the same comparisons for the NACA 0012 airfoil at Mach 0.8 and  $1.25^\circ$  angle of attack. In each of these cases the two schemes give more or less identical results, with the switched scheme converging a little faster. In other numerical tests, however, the switched scheme has been found to provide less reliable resolution of very weak shock waves.

Figures 15 and 16 show applications of the SLIP

scheme with characteristic splitting to two airfoils which had previously been found to have non-unique solutions in calculations using the JST scheme with scalar diffusion [10]. The non-uniqueness is confirmed in these calculations, supporting the belief that these airfoils truly admit non-unique Euler solutions.

Finally, Figure 17 shows a three-dimensional Euler solution for the ONERA M6 wing at Mach 0.840 and an angle of attack of  $3.06^\circ$  calculated on a  $192 \times 32 \times 48$  mesh with O-O topology using the SLIP scheme with characteristic splitting. This again verifies the non-oscillatory character of the solution and sharp resolution of shock waves.

These numerical experiments confirm the theory of local extremum diminishing (LED) schemes, as it has been set forth in this paper. The following are the main conclusions of this study:

1. The scalar diffusion that has been widely used can be significantly improved by the addition of a pressure term as defined in the CUSP formulation. Sharp discrete shocks are then obtained at high Mach numbers, and rapid multigrid convergence at all Mach numbers.
2. The use of a split diffusive flux corresponding to the characteristic fields with Roe averaging improves the resolution of shocks in the transonic range, particularly when they are weak.
3. The switched Jameson-Schmidt-Turkel (JST) scheme with the improved switch defined by Equation (8c) is effective for steady state calculations in a wide Mach range.
4. The symmetric limited positive (SLIP) scheme defined by equation (9) is a computationally efficient scheme for oscillation control in both steady and unsteady flow. The accuracy is significantly affected by the choice of limiter.
5. Higher order SLIP schemes can be constructed and can improve the accuracy.

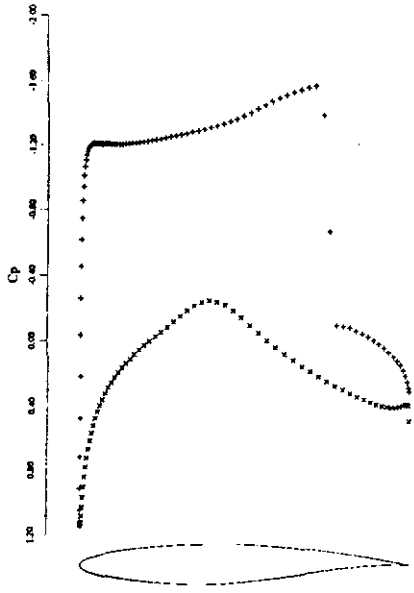
## Acknowledgment

This work has benefited from the generous support of ARPA under Grant No. N00014-92-J-1796, AFOSR under Grant No. AFOSR-91-0391, and IBM.

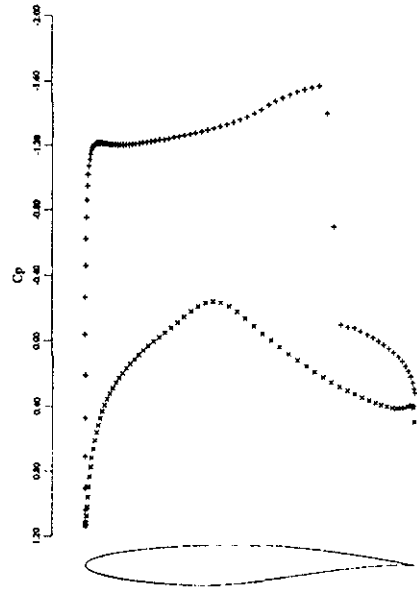
## References

- [1] P. Arminjon and A. Dervieux. Construction of TVD-like artificial viscosities on 2-dimensional arbitrary FEM grids. *INRIA Report 1111*, October 1989.
- [2] J.P. Boris and D.L. Book. Flux corrected transport, 1 SHASTA, a fluid transport algorithm that works. *Journal of Computational Physics*, 11:38-69, 1973.
- [3] R.J. Busch, Jr. Computational fluid dynamics in the design of the Northrop/McDonnell Douglas YF-23 ATF prototype. *AIAA paper 91-1627*, AIAA 21st Fluid Dynamics, Plasmadynamics & Lasers Conference, Honolulu, Hawaii, 1991.
- [4] J.D. Denton. An improved time marching method for turbomachinery flow calculations. *Journal of Engineering for Gas Turbines and Power*, 105, 1983.
- [5] A. Harten. High resolution schemes for hyperbolic conservation laws. *Journal of Computational Physics*, 49:357-393, 1983.
- [6] A. Jameson. Solution of the Euler equations for two dimensional transonic flow by a multigrid method. *Applied Mathematics and Computations*, 13:327-356, 1983.
- [7] A. Jameson. A non-oscillatory shock capturing scheme using flux limited dissipation. MAE Report 1653, Princeton University, Princeton, New Jersey, April 1984. Published in *Lectures in Applied Mathematics*, B.E. Engquist, S. Osher, and R.C.J. Somerville, editor, A.M.S., Part 1, 22:345-370, 1985.
- [8] A. Jameson. Multigrid algorithms for compressible flow calculations. In W. Hackbusch and U. Trottenberg, editors, *Lecture Notes in Mathematics, Vol. 1228*, pages 166-201. Proceedings of the 2nd European Conference on Multigrid Methods, Cologne, 1985, Springer-Verlag, 1986.
- [9] A. Jameson. Successes and challenges in computational aerodynamics. *AIAA paper 87-1184-CP*, AIAA 8th Computational Fluid Dynamics Conference, Honolulu, Hawaii, 1987.
- [10] A. Jameson. Airfoils admitting non-unique solutions of the Euler equations. *AIAA paper 91-1625*, AIAA 22nd Fluid Dynamics, Plasmadynamics & Lasers Conference, Honolulu, Hawaii, June 1991.
- [11] A. Jameson, T.J. Baker, and N.P. Weatherill. Calculation of inviscid transonic flow over a complete aircraft. *AIAA paper 86-0103*,

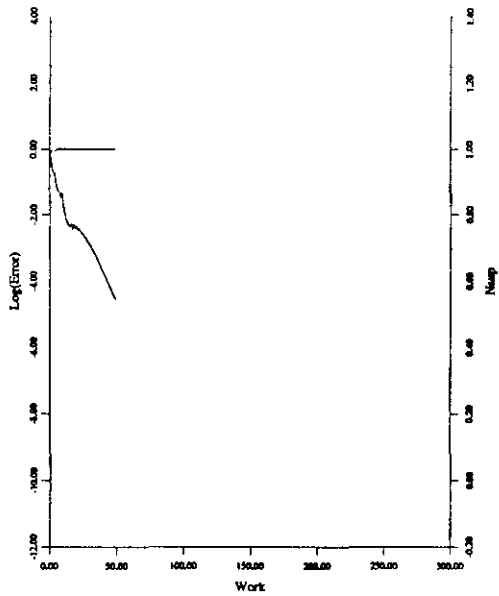
- AIAA 24th Aerospace Sciences Meeting, Reno, Nevada, January 1986.
- [12] A. Jameson, W. Schmidt, and E. Turkel. Numerical solutions of the Euler equations by finite volume methods with Runge-Kutta time stepping schemes. *AIAA paper 81-1259*, January 1981.
- [13] B. Laney and D.A. Caughey. Extremum control II: Semi-discrete approximations to conservation laws. *AIAA paper 91-0632*, AIAA 29th Aerospace Sciences Meeting, Reno, Nevada, January 1991.
- [14] B. Van Leer. Flux vector splitting for the Euler equations. In E. Krause, editor, *Proceedings of the 8th International Conference on Numerical Methods in Fluid Dynamics*, pages 507-512, Aachen, 1982.
- [15] M-S. Liou and C.J. Steffen. A new flux splitting scheme. *NASA-TM 104452*, 1991. Accepted for publication in the *Journal of Computational Physics*.
- [16] S. Osher and F. Solomon. Upwind difference schemes for hyperbolic systems of conservation laws. *Mathematics and Computing*, 38:339-374, 1982.
- [17] P.L. Roe. Approximate Riemann solvers, parameter vectors, and difference schemes. *Journal of Computational Physics*, 43:357-372, 1981.
- [18] C. Shu and S. Osher. Efficient implementation of essentially non-oscillatory shock-capturing schemes. *Journal of Computational Physics*, 77:439-471, 1988.
- [19] G.A. Sod. A survey of several finite difference methods for systems of nonlinear hyperbolic conservation laws. *Journal of Computational Physics*, 27:1-31, 1978.
- [20] J.L. Steger and R.F. Warming. Flux vector splitting of the inviscid gas dynamic equations with applications to finite difference methods. *Journal of Computational Physics*, 40:263-293, 1981.
- [21] R.C. Swanson and E. Turkel. On central-difference and upwind schemes. *Journal of Computational Physics*, 101:297-306, 1992.
- [22] P.K. Sweby. High resolution schemes using flux limiters for hyperbolic conservation laws. *Journal of Numerical Analysis*, 21:995-1011, 1984.
- [23] S. Tatsumi, L. Martinelli, and A. Jameson. Design, implementation, and validation of flux limited schemes for the solution of the compressible Navier-Stokes equations. *Abstract*, Submitted to AIAA 32nd Aerospace Sciences Meeting, Reno, Nevada, January 1994.
- [24] S.T. Zalesak. Fully multidimensional flux-corrected transport algorithms for fluids. *Journal of Computational Physics*, 31:335-362, 1979.



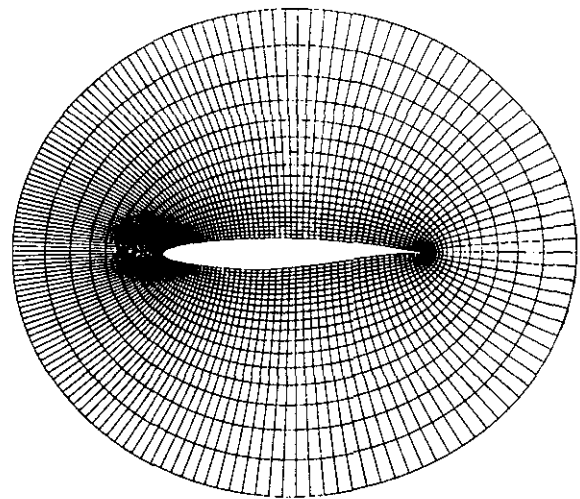
5a:  $C_p$  after 12 Cycles.  
 $C_l = 1.1262, C_d = 0.0467.$



5b:  $C_p$  after 50 Cycles.  
 $C_l = 1.1284, C_d = 0.0470.$

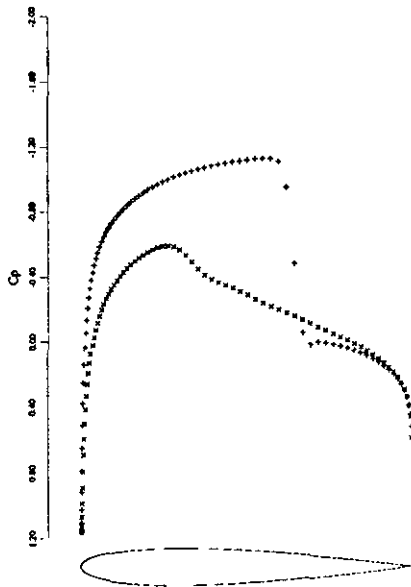


5c: Convergence.

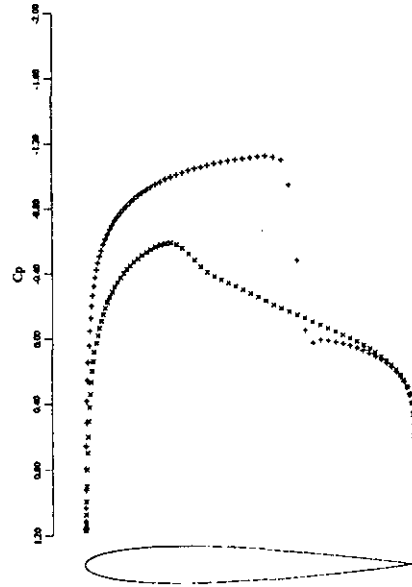


5d: Grid.

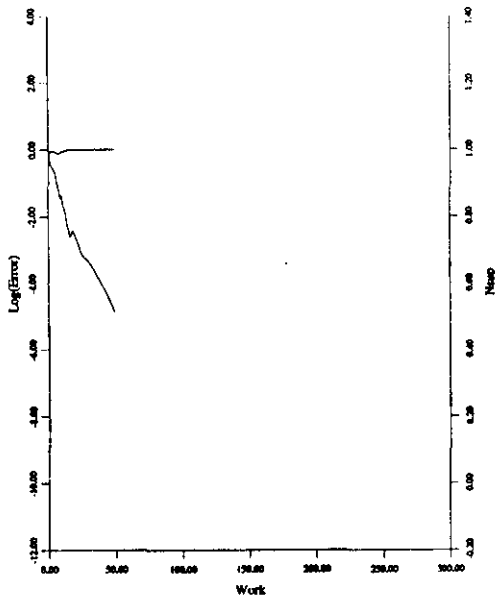
Figure 5: RAE 2822. Mach 0.750, Angle of Attack  $3^\circ$ ,  $160 \times 32$  Mesh.  
 CUSP Scheme.



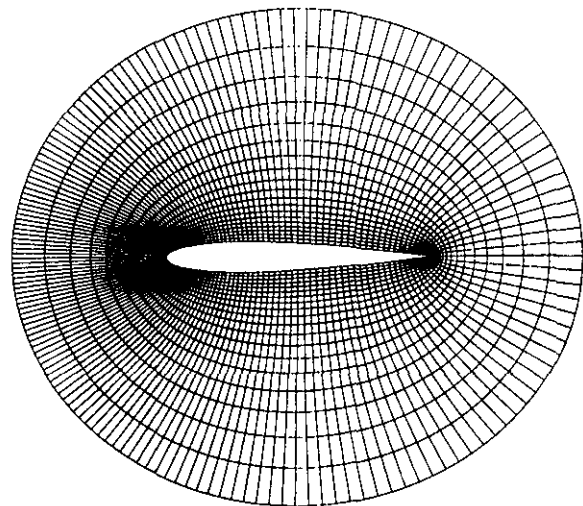
6a:  $C_p$  after 12 Cycles.  
 $C_l = 0.3653$ ,  $C_d = 0.0234$ .



6b:  $C_p$  after 50 Cycles.  
 $C_l = 0.3665$ ,  $C_d = 0.0234$ .

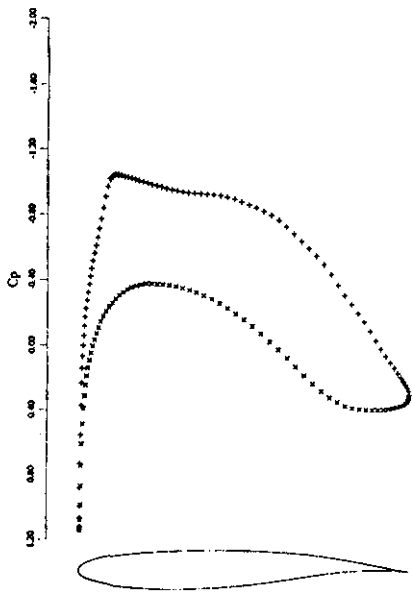


6c: Convergence.

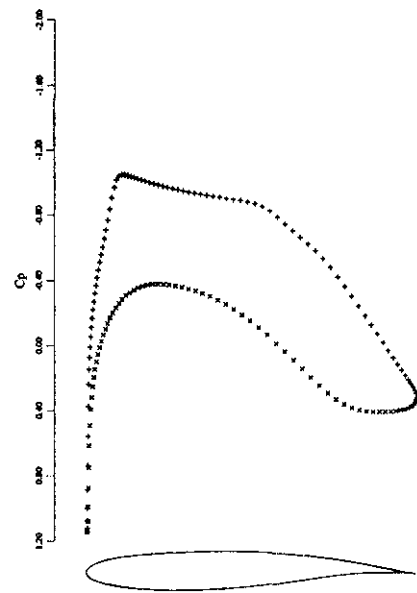


6d: Grid.

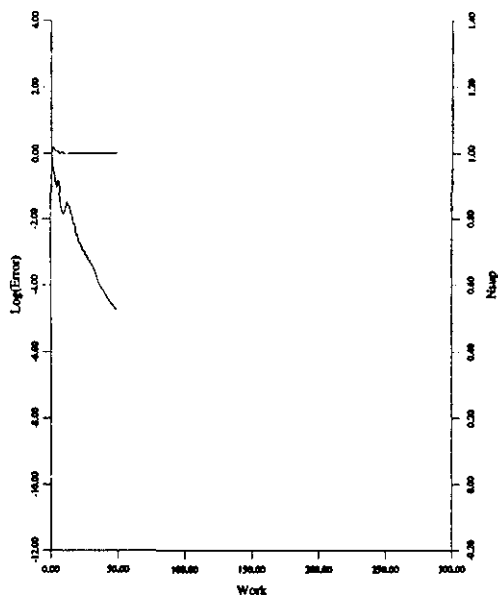
Figure 6: NACA 0012. Mach 0.800, Angle of Attack 1.25°, 160×32 Mesh.  
 CUSP Scheme.



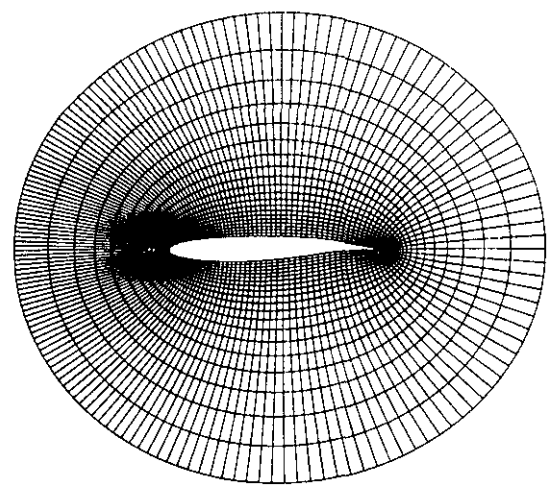
7a:  $C_p$  after 12 Cycles.  
 $C_l = 0.6309$ ,  $C_d = 0.0001$ .



7b:  $C_p$  after 50 Cycles.  
 $C_l = 0.6311$ ,  $C_d = 0.0000$ .

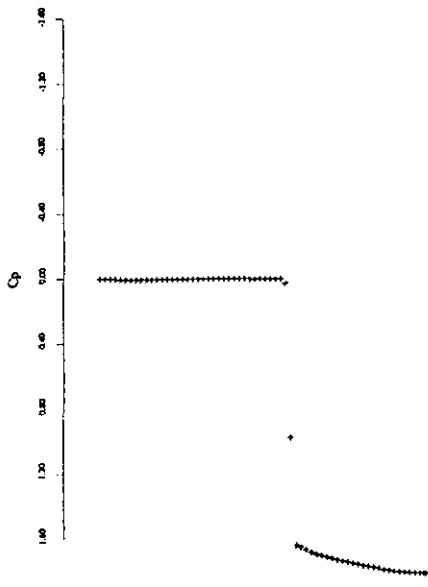


7c: Convergence.

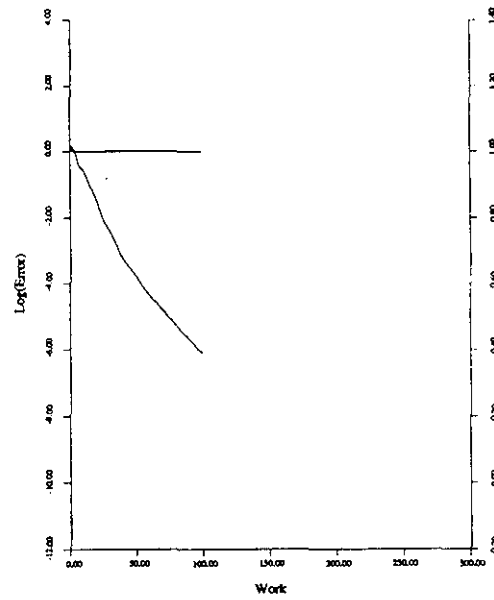


7d: Grid.

Figure 7: KORN Airfoil. Mach 0.750, Angle of Attack  $0^\circ$ ,  $160 \times 32$  Mesh.  
 CUSP Scheme.

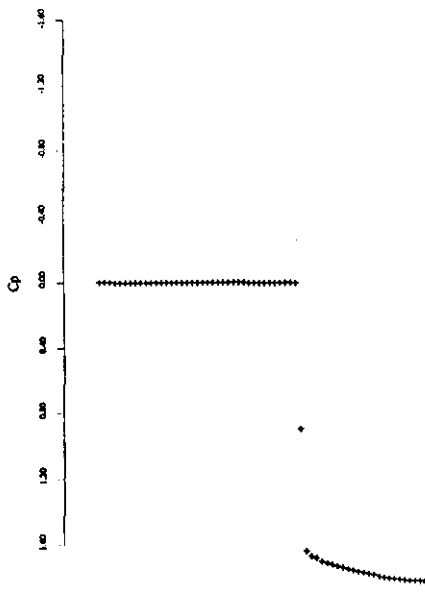


8a:  $C_p$  on the Centerline in Front of the Body.

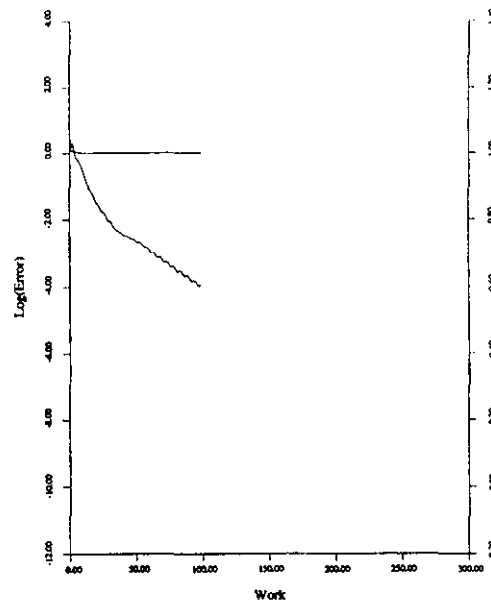


8b: Convergence.

Figure 8: Bluff Body. Mach 8,  $160 \times 64$  Mesh.  
CUSP Scheme.

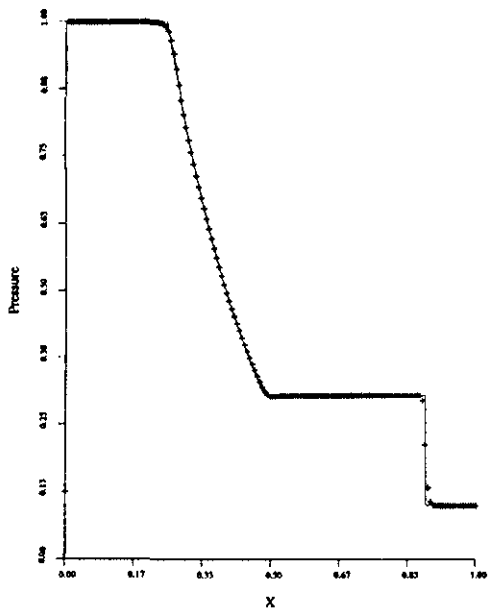


9a:  $C_p$  on the Centerline in Front of the Body.

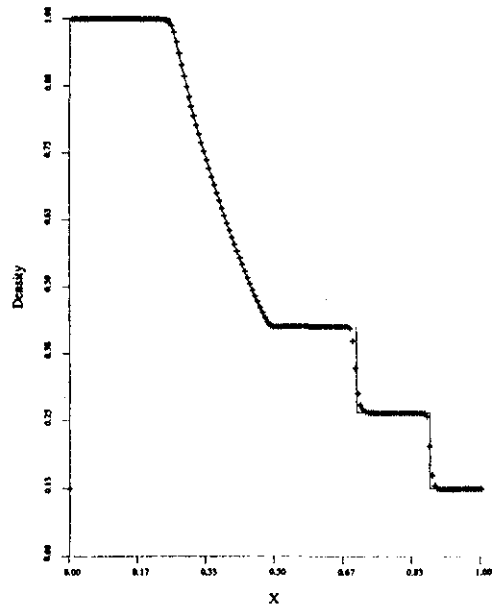


9b: Convergence.

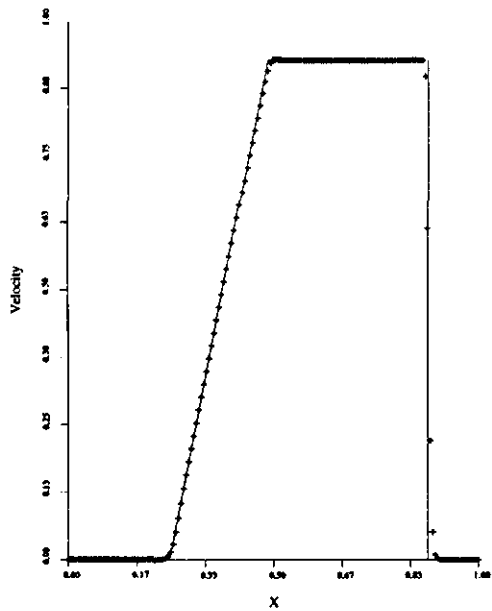
Figure 9: Bluff Body. Mach 20,  $160 \times 64$  Mesh.  
CUSP Scheme.



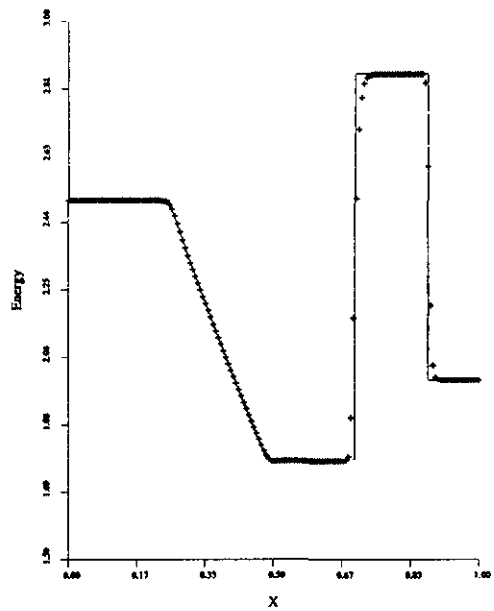
10a: Pressure.



10b: Density.

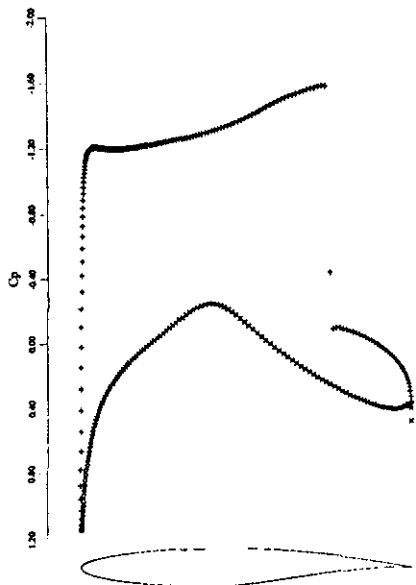


10c: Velocity.

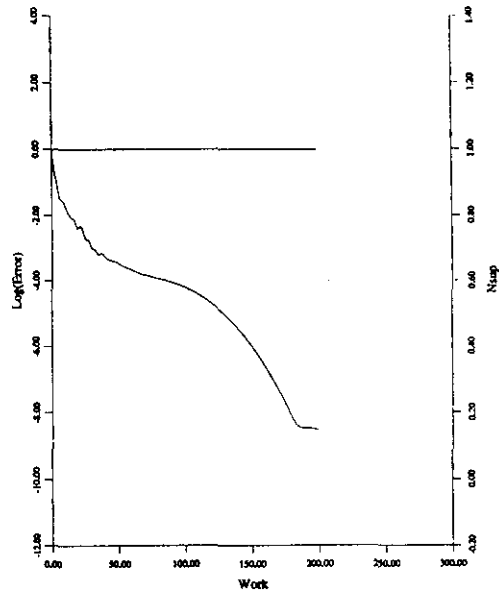


10d: Energy.

Figure 10: Shock Tube Problem using SLIP Scheme with Pressure and Density Ratios of 10.0 and 8.0, respectively. Computed Results (+) are Compared with Theory (—) for 160 Equally Spaced Mesh Points.

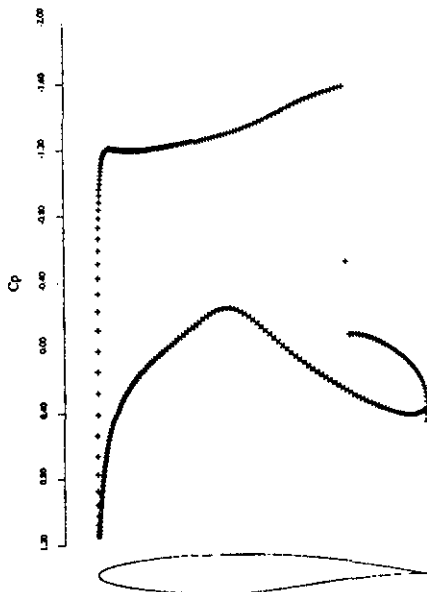


11a:  $C_p$ .  
 $C_l = 1.1167, C_d = 0.0455$ .

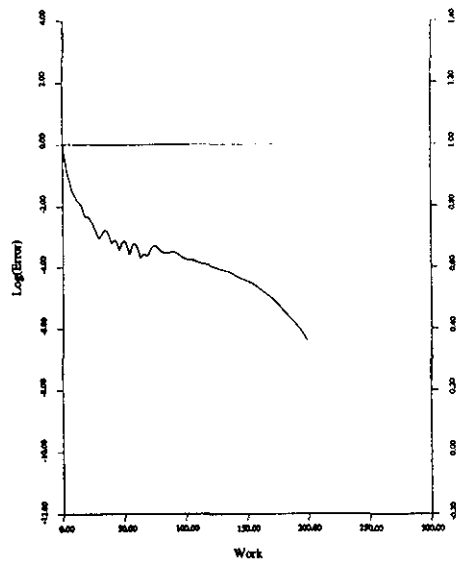


11b: Convergence.

Figure 11: RAE 2822 with JST Scheme and Characteristic Splitting.  
 Mach 0.750, Angle of Attack  $3^\circ$ ,  $320 \times 64$  Mesh.

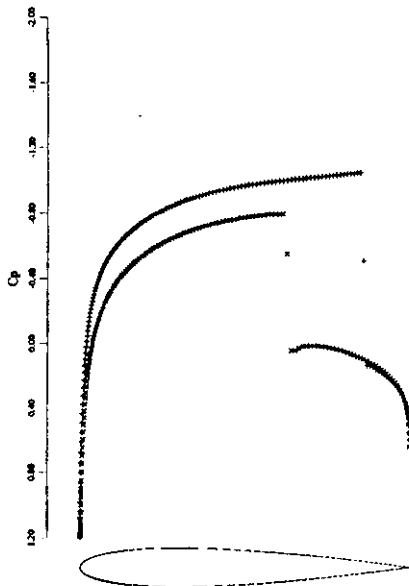


12a:  $C_p$ .  
 $C_l = 1.1194, C_d = 0.0456$ .

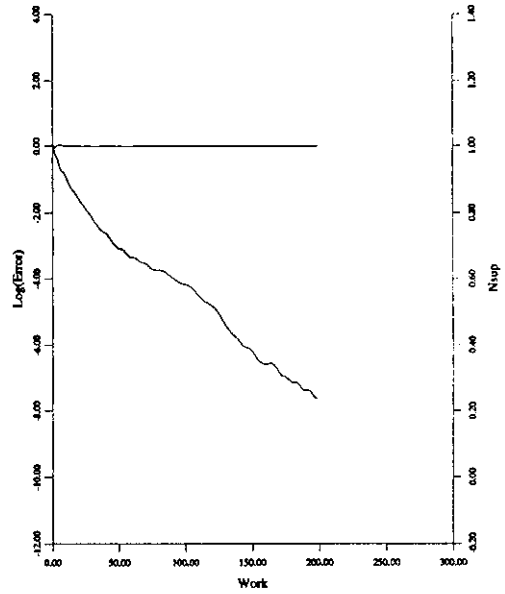


12b: Convergence.

Figure 12: RAE 2822 with SLIP Scheme and Characteristic Splitting.  
 Mach 0.750, Angle of Attack  $3^\circ$ ,  $320 \times 64$  Mesh.

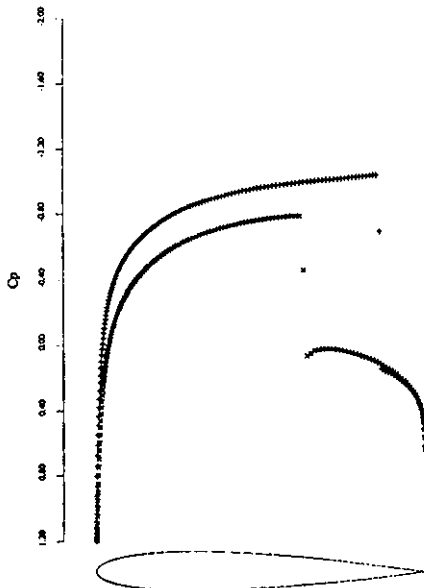


13a:  $C_p$ .  
 $C_l = 0.3729$ ,  $C_d = 0.0575$ .

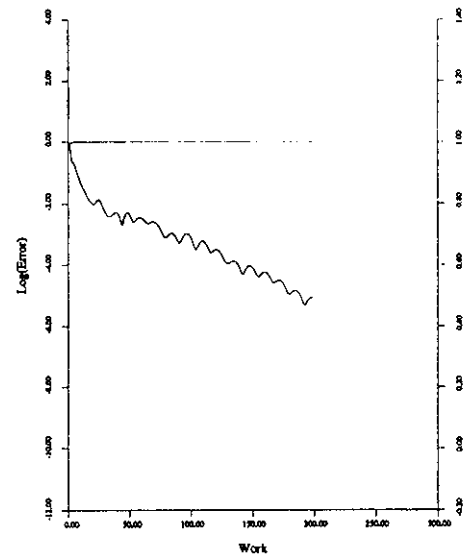


13b: Convergence.

Figure 13: NACA 0012 with JST Scheme and Characteristic Splitting.  
Mach 0.850, Angle of Attack  $1^\circ$ ,  $320 \times 64$  Mesh.

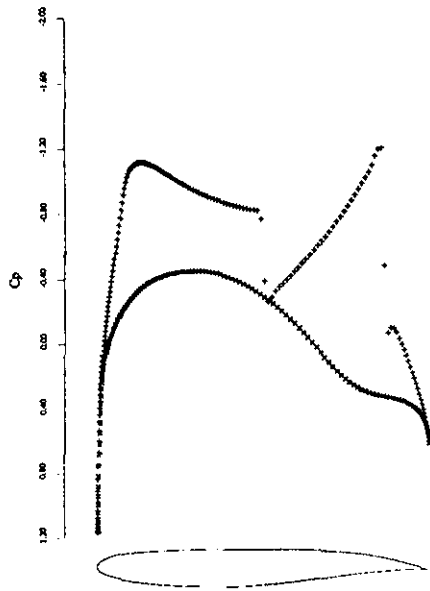


14a:  $C_p$ .  
 $C_l = 0.3768$ ,  $C_d = 0.0576$ .

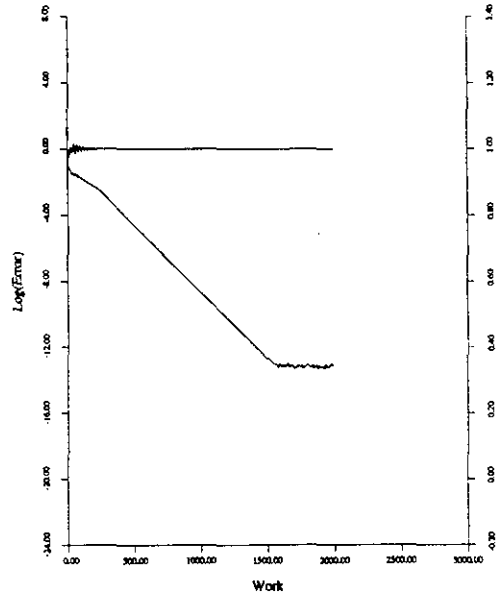


14b: Convergence.

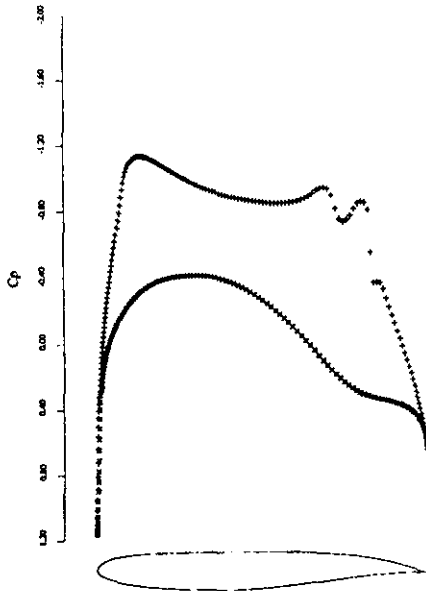
Figure 14: NACA 0012 with SLIP Scheme and Characteristic Splitting.  
Mach 0.850, Angle of Attack  $1^\circ$ ,  $320 \times 64$  Mesh.



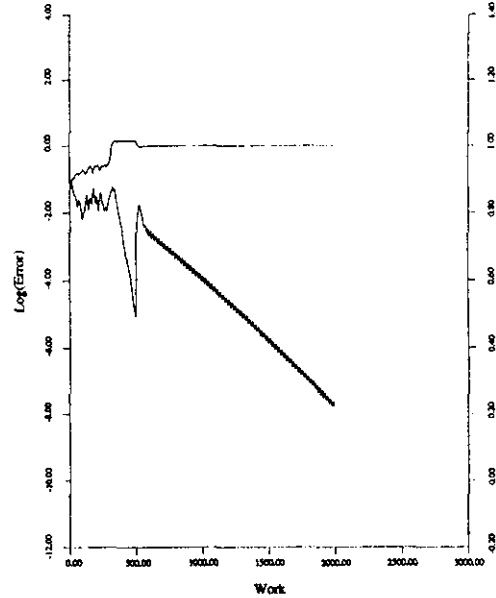
15a:  $C_p$ .  
 $C_l = 0.5696$ ,  $C_d = 0.0068$ .



15b: Convergence.

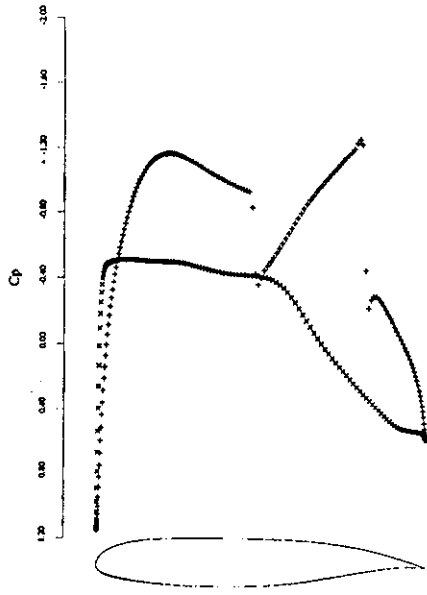


15c:  $C_p$ .  
 $C_l = 0.6575$ ,  $C_d = 0.0016$ .

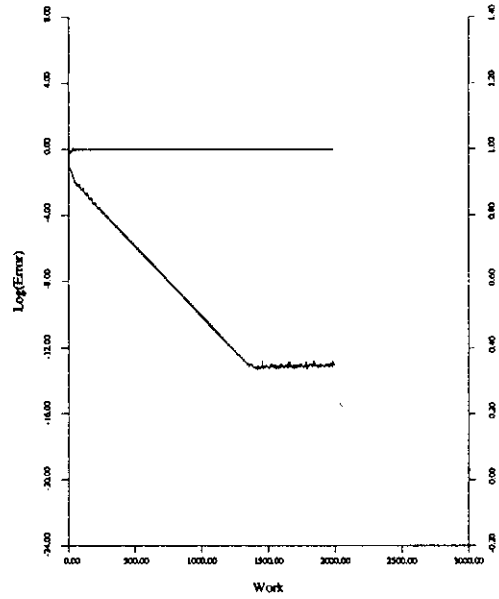


15d: Convergence.

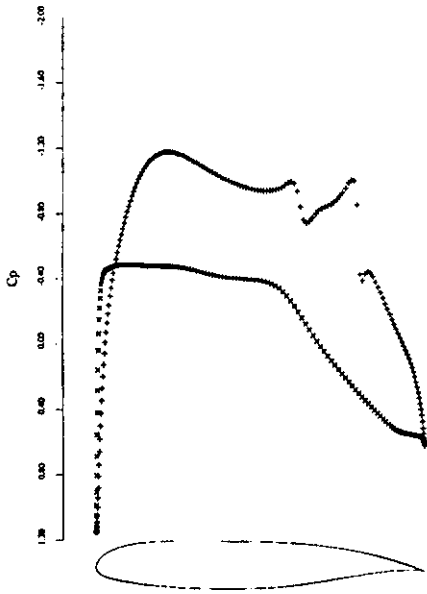
Figure 15: J-78 Airfoil: Non-Unique Solutions.  
 SLIP Scheme with Characteristic Splitting.  
 Mach 0.780, Angle of Attack  $-0.60^\circ$ ,  $321 \times 65$  Mesh.



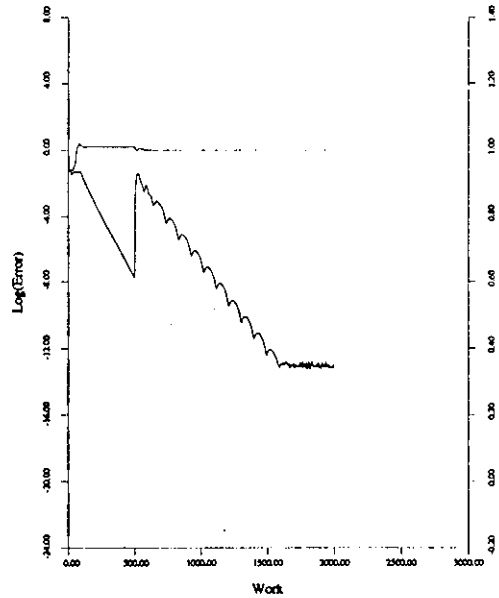
16a:  $C_p$ .  
 $C_l = 0.5502$ ,  $C_d = 0.0055$ .



16b: Convergence.

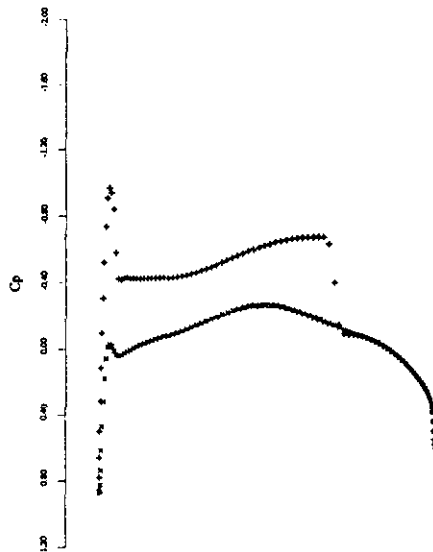


16c:  $C_p$ .  
 $C_l = 0.5988$ ,  $C_d = 0.0013$ .

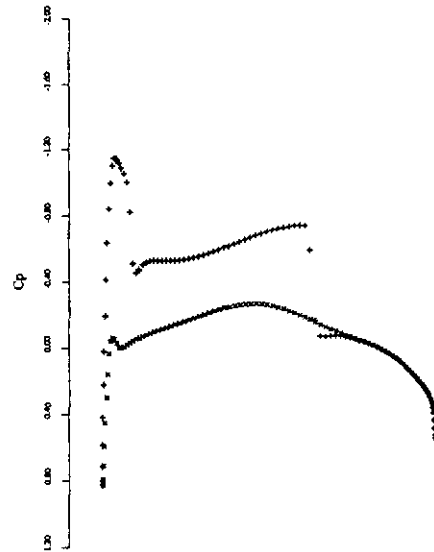


16d: Convergence.

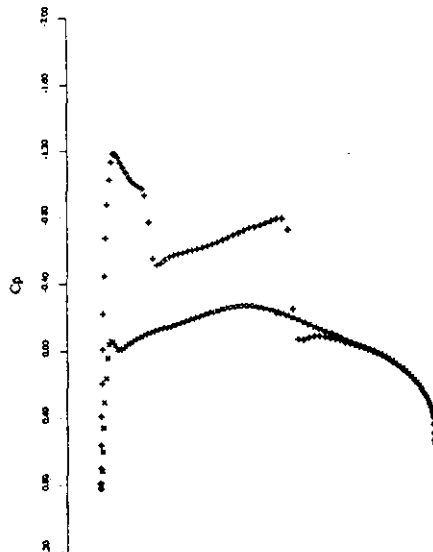
Figure 16: GAW75-06-15 Airfoil: Non-Unique Solutions.  
 SLIP Scheme with Characteristic Splitting.  
 Mach 0.750, Angle of Attack  $-2.250^\circ$ ,  $321 \times 65$  Mesh.



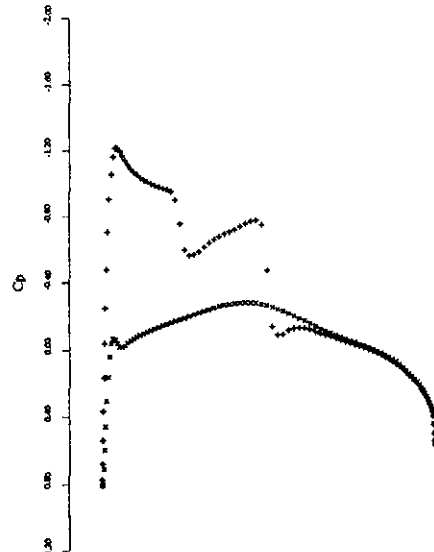
17a: 10.9% Span.  
 $C_l = 0.2864$ ,  $C_d = 0.0281$ .



17b: 29.7% Span.  
 $C_l = 0.3066$ ,  $C_d = 0.0158$ .



17c: 48.4% Span.  
 $C_l = 0.3176$ ,  $C_d = 0.0084$ .



17d: 67.2% Span.  
 $C_l = 0.3097$ ,  $C_d = 0.0017$ .

Figure 17: Onera M6 Wing with SLIP Scheme and Characteristic Splitting.  
Mach 0.840, Angle of Attack 3.06°, 192×32×48 Mesh.  
 $C_L = 0.2914$ ,  $C_D = 0.0117$ .